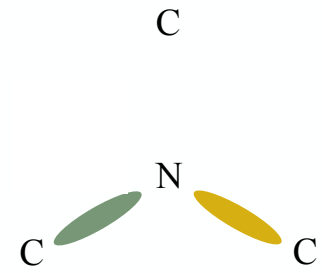
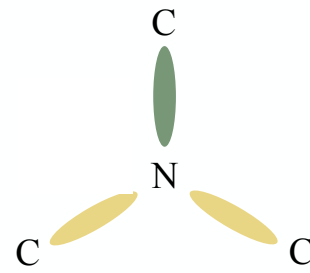
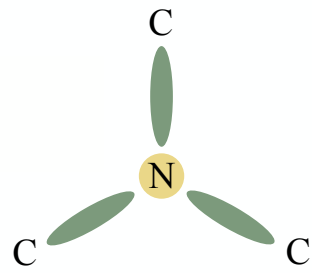
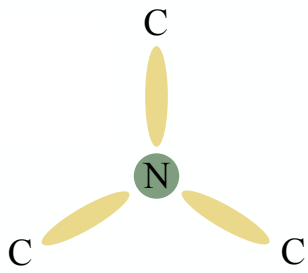


The NV center in diamond:
Spectroscopy at room temperature
**Optically detected magnetic
resonance**

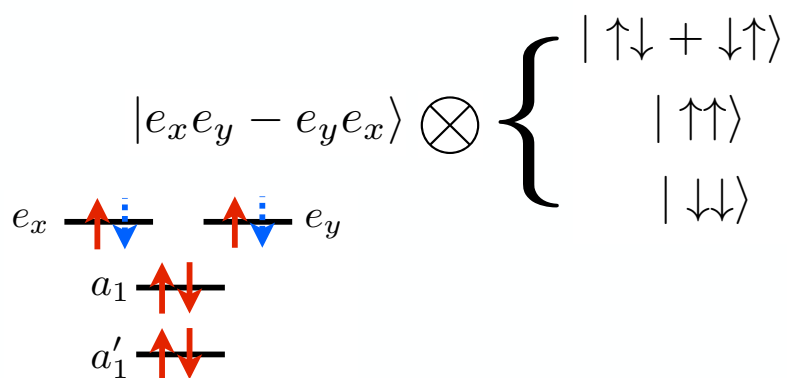
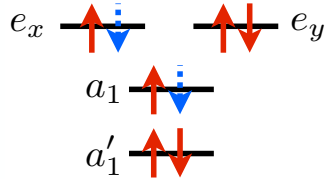
Spectroscopy of the NV center



orbital \otimes spin

$$|Y\rangle = |ae_y - e_ya\rangle \otimes \begin{cases} |\uparrow\downarrow + \downarrow\uparrow\rangle \\ |\uparrow\uparrow\rangle \\ |\downarrow\downarrow\rangle \end{cases}$$

$$|X\rangle = |ae_x - e_xa\rangle \otimes \begin{cases} |\uparrow\downarrow + \downarrow\uparrow\rangle \\ |\uparrow\uparrow\rangle \\ |\downarrow\downarrow\rangle \end{cases}$$



selection rule
for optical transition

$$\langle \psi_f | \vec{d} \cdot \vec{E} | \psi_i \rangle \neq 0$$

$$\langle a | \vec{x} \cdot \hat{r} | e_x \rangle = \langle a | \vec{y} \cdot \hat{r} | e_y \rangle \neq 0$$

What is the influence of
the electron spin ?

Hamiltonian – Difference with atomic physics

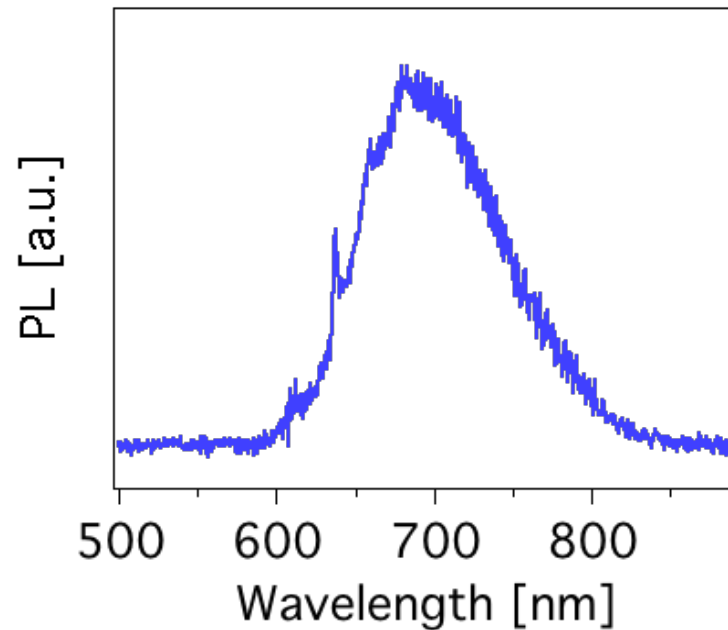
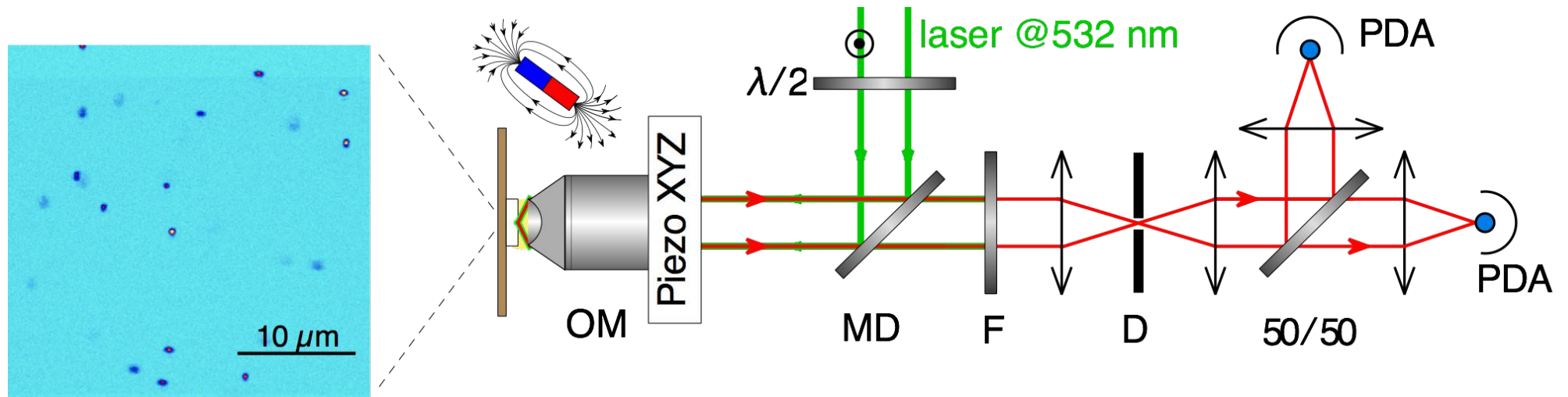
$$H = H_{\text{spin-orbit}} + H_{\text{spin-spin}} + H_{\text{strain}}$$

- In alkali atoms, spin-orbit interaction is \sim THz
Total spin projection can be optically modified.
- In the NV center, spin-orbit coupling split the excited orbitals by \sim 5 GHz.
At low T, transitions that alter m_s are allowed leading to spin-photon entanglement schemes.
- At room temperature, phonons induce orbital averaging in the excited state or strain is the dominant perturbation.

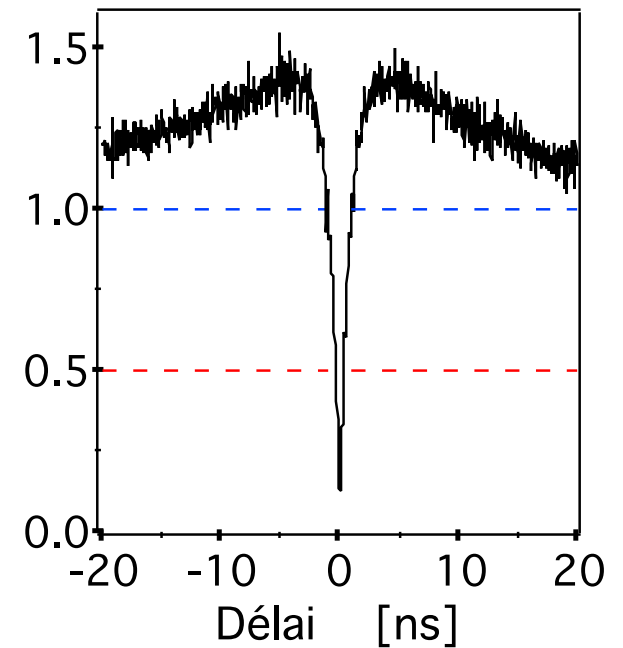
→ selection rule $\Delta m_s = 0$

→ 2 incoherent optical dipoles \perp NV axis

Confocal microscopy for single-emitter detection

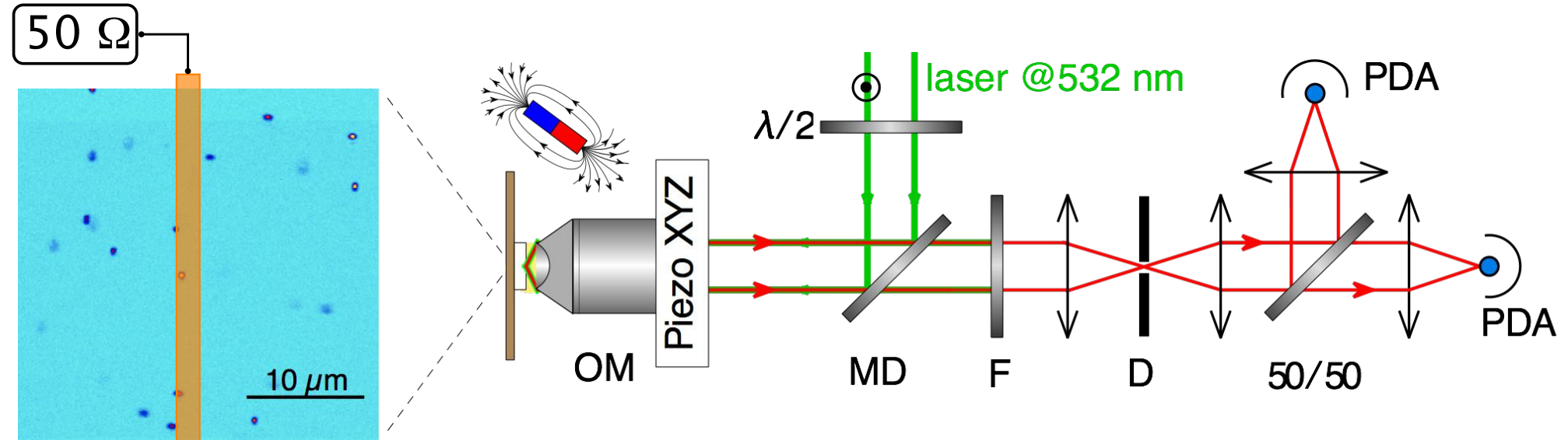


NV⁻ center

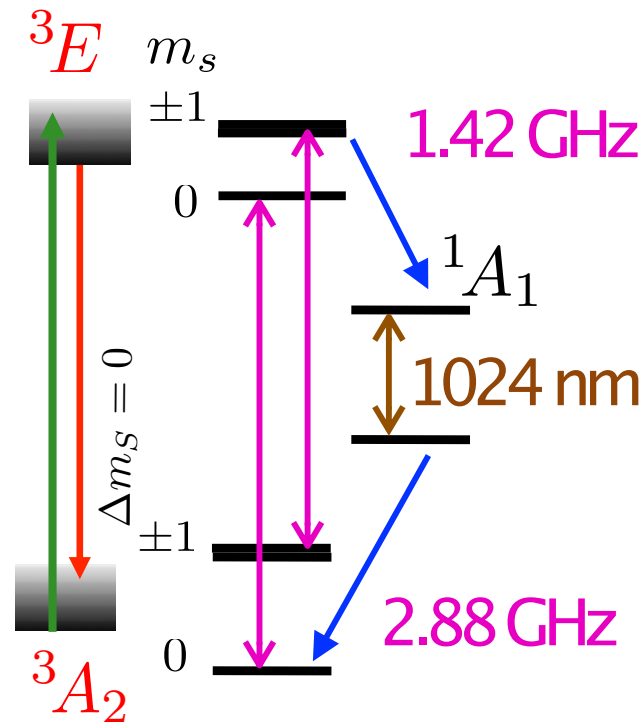
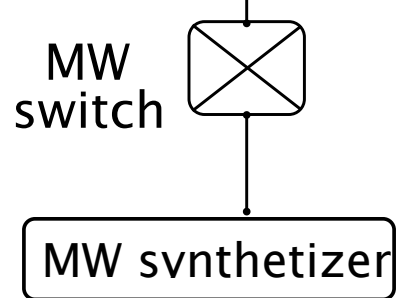


single emitter

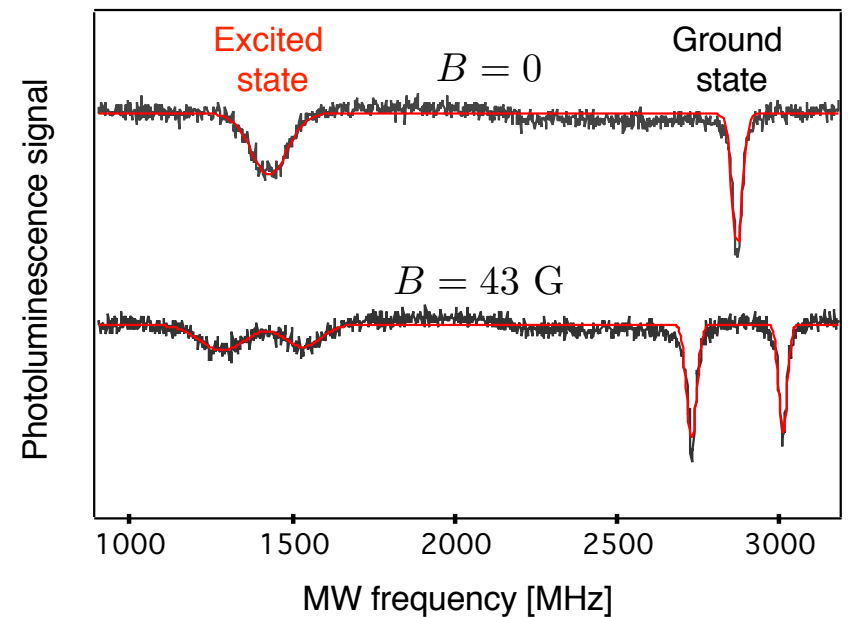
Optical polarization and luminescence



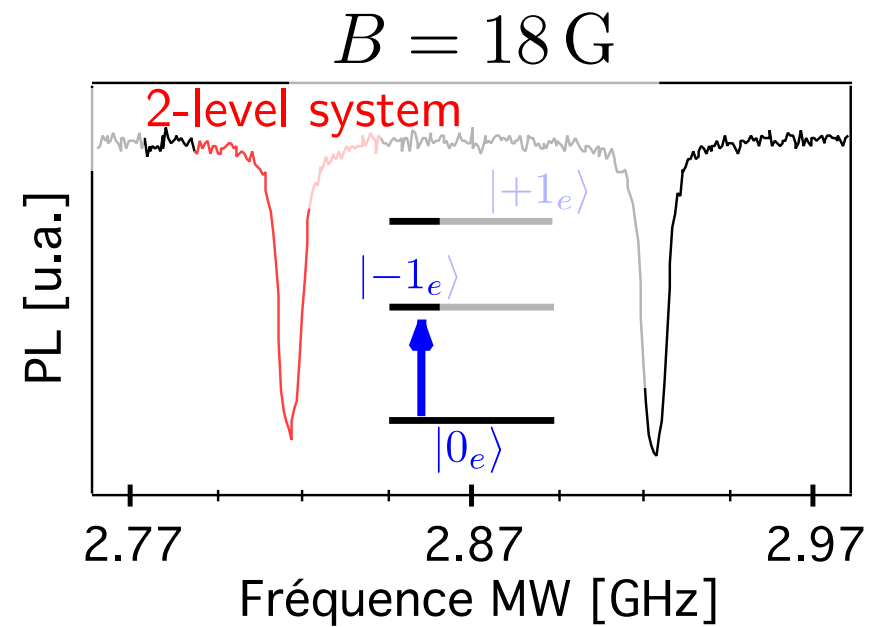
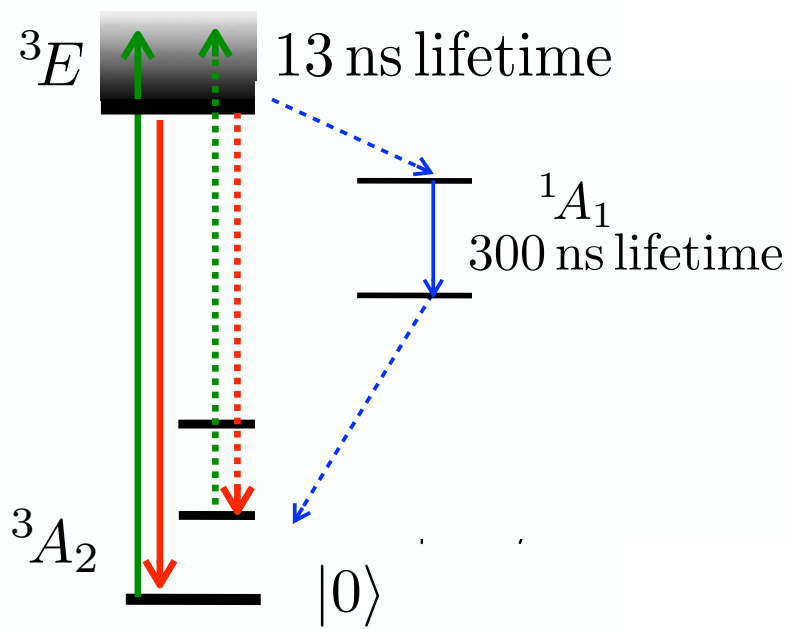
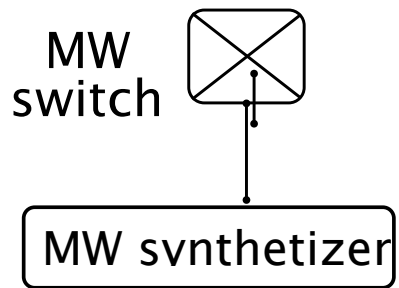
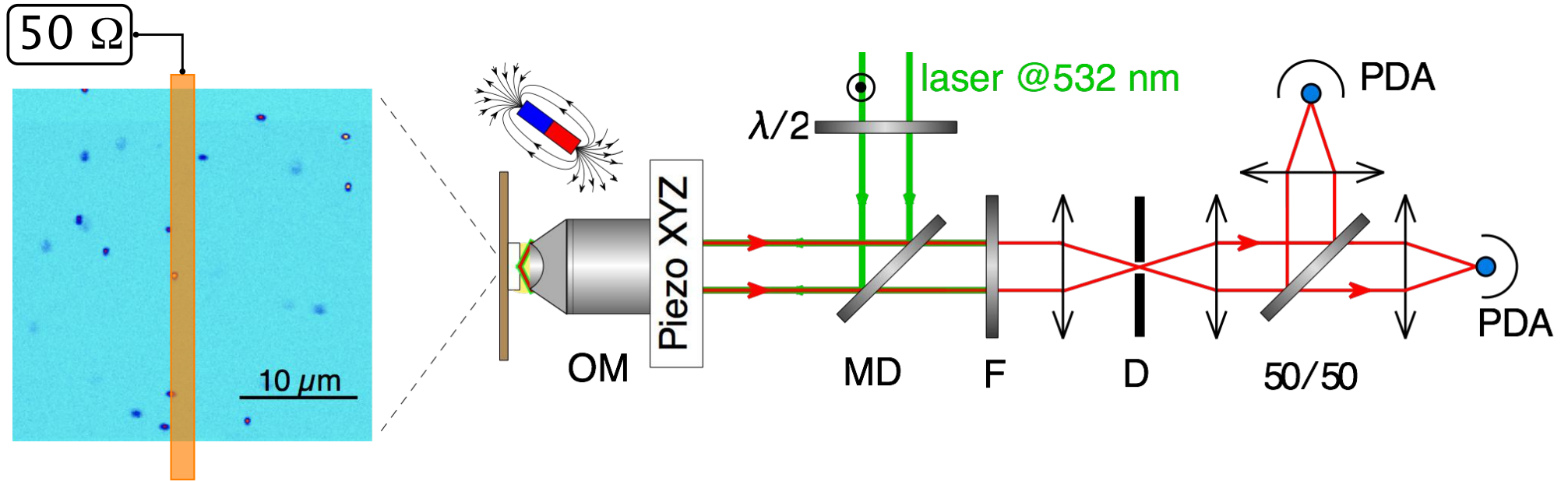
Room temperature



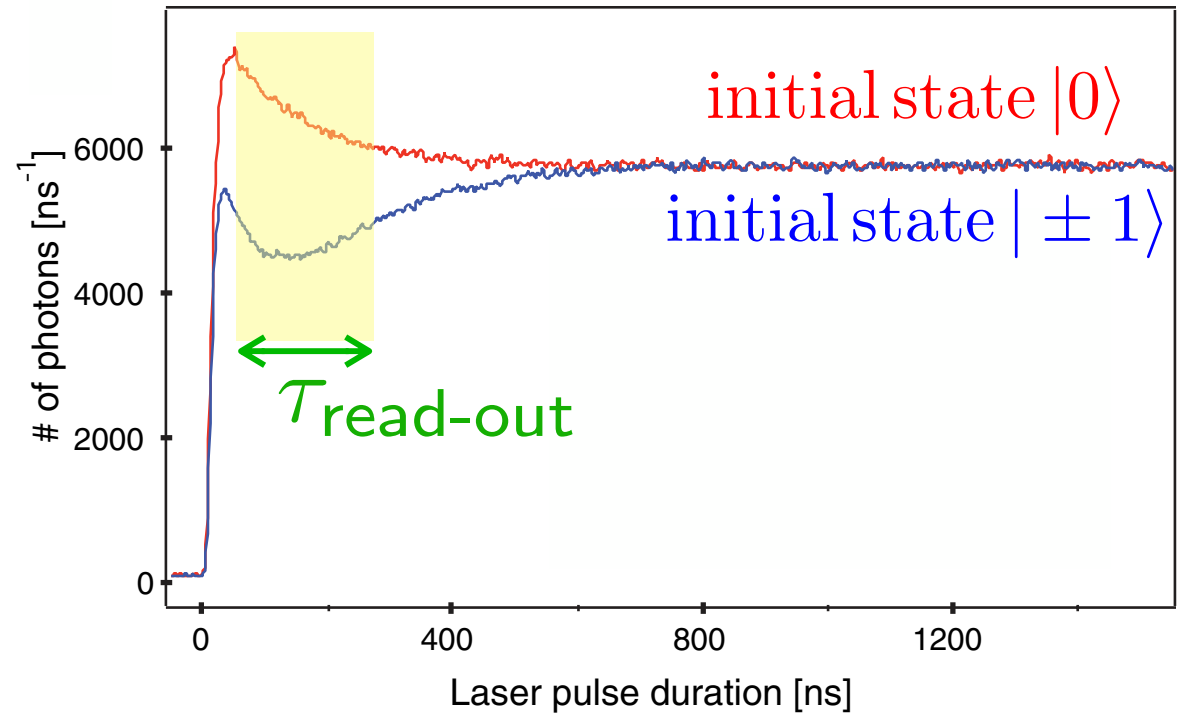
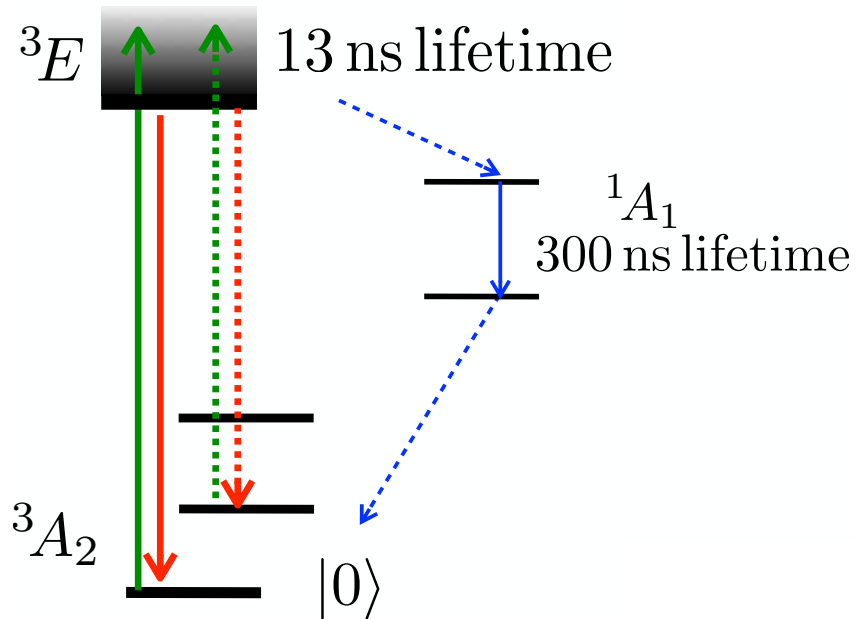
- 3E excited state: $\tau \simeq 13$ ns
- 1A_1 metastable level: $\tau \simeq 200$ ns



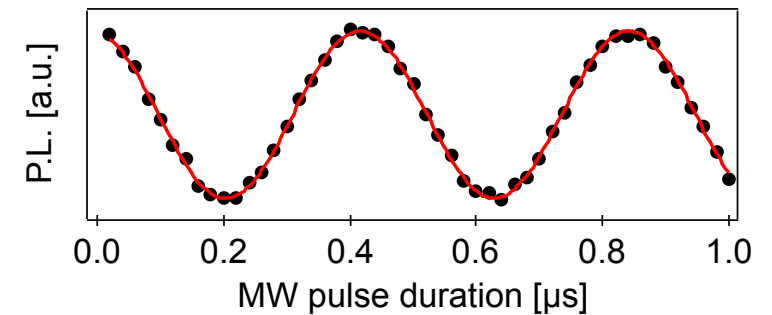
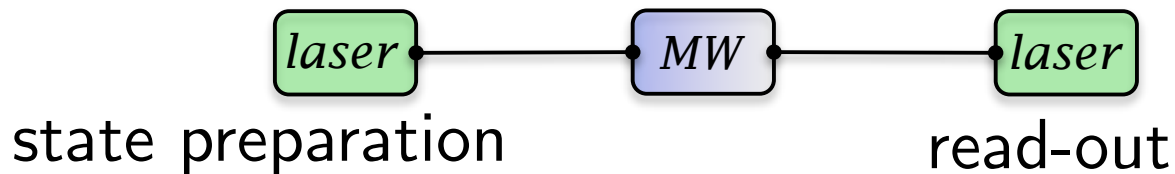
Spin-based 2-level quantum system



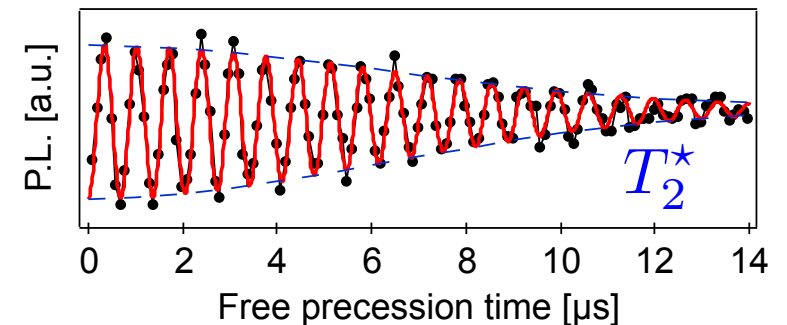
$(|0\rangle, |1\rangle)$ quantum states



● Rabi oscillation de Rabi



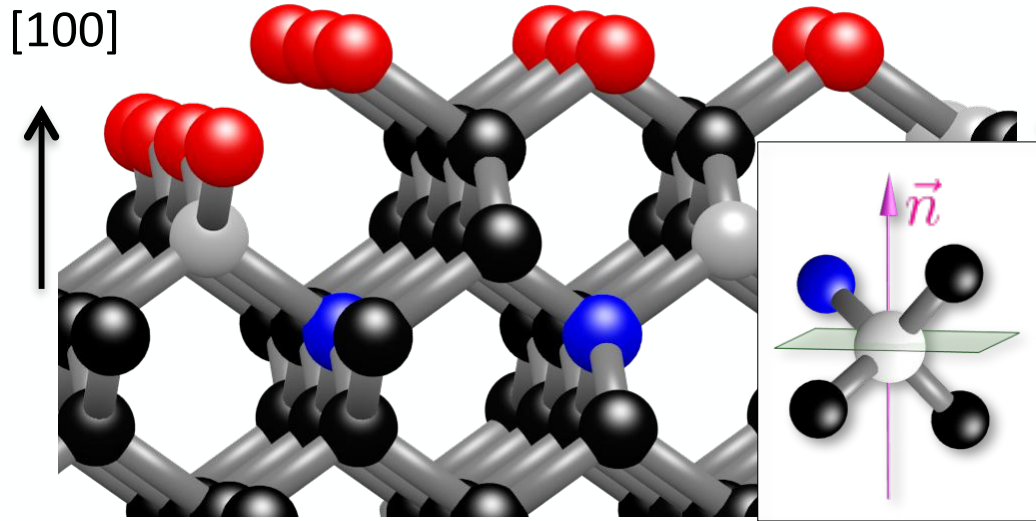
● Ramsay fringes



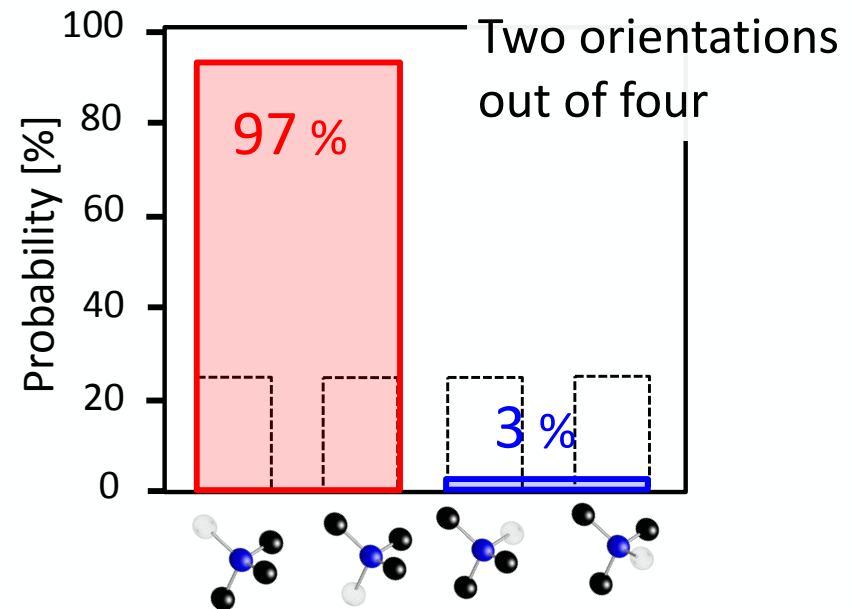
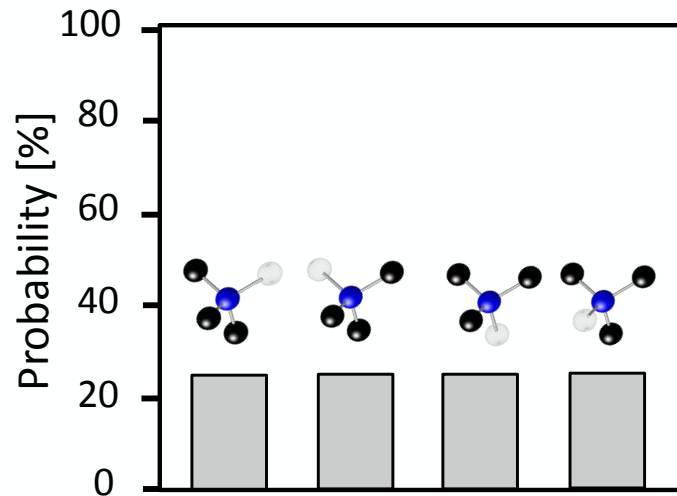
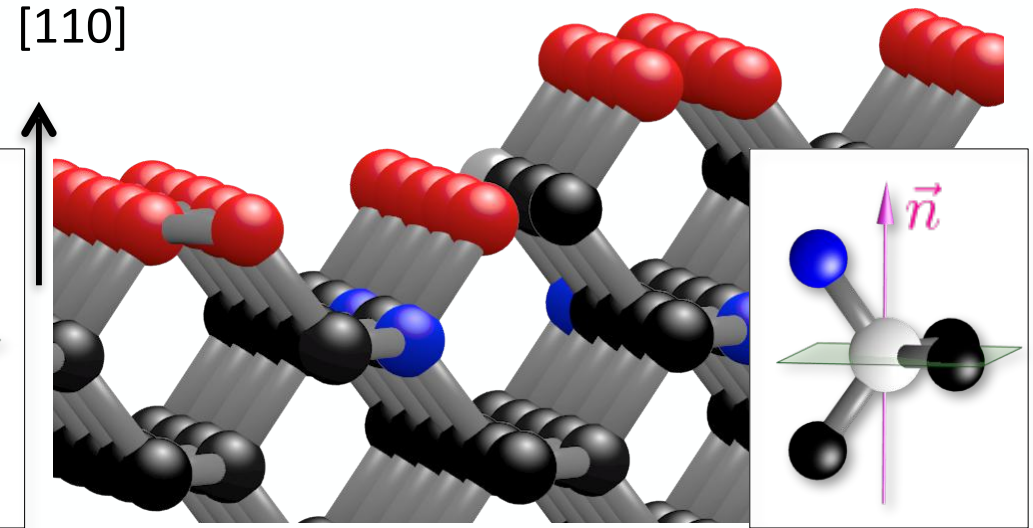
NV center orientation is the intrinsic quantization axis



(100)-oriented growth:



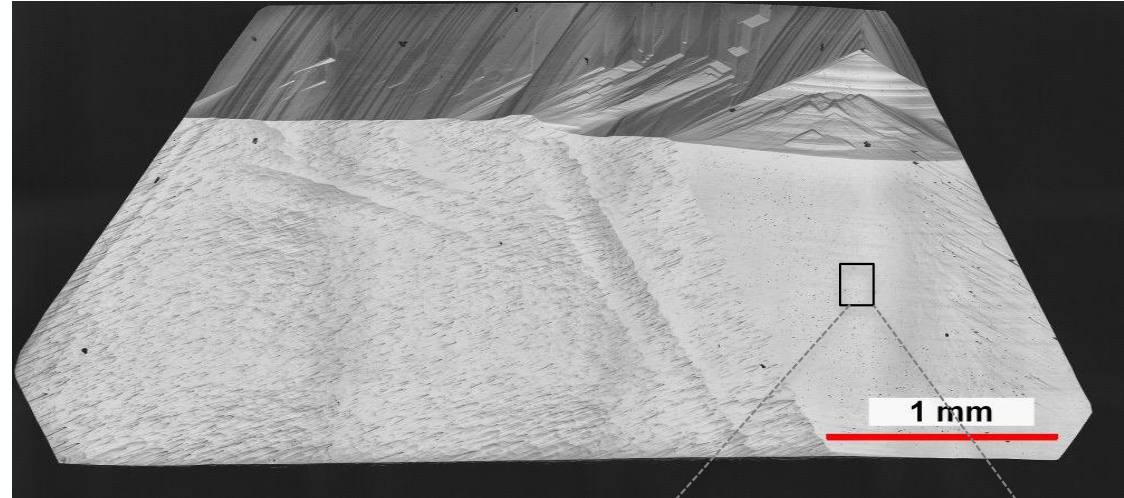
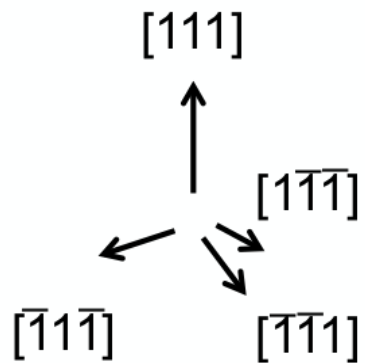
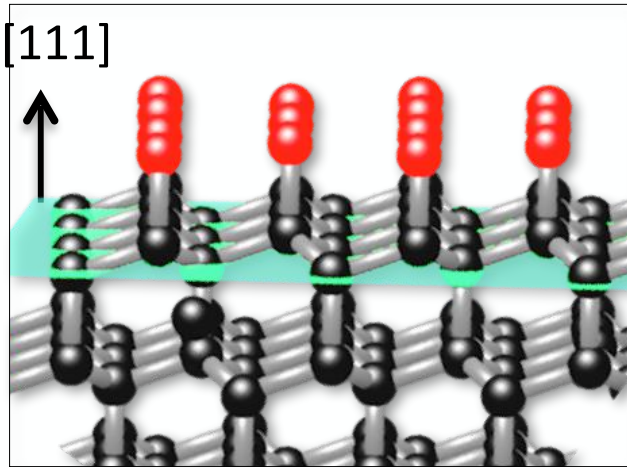
(110)-oriented growth:



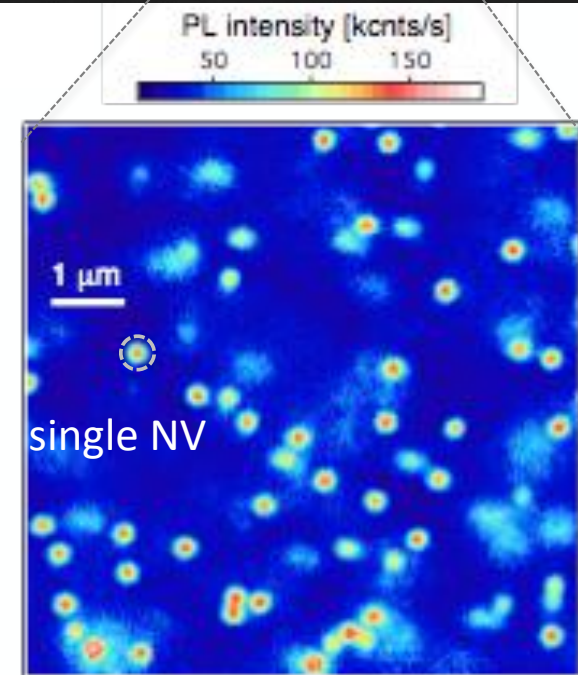
* Pham, et al., Phys. Rev. B 86, 121202(R) (2012).

** Edmonds, et al., Phys. Rev. B 86, 035201 (2012).

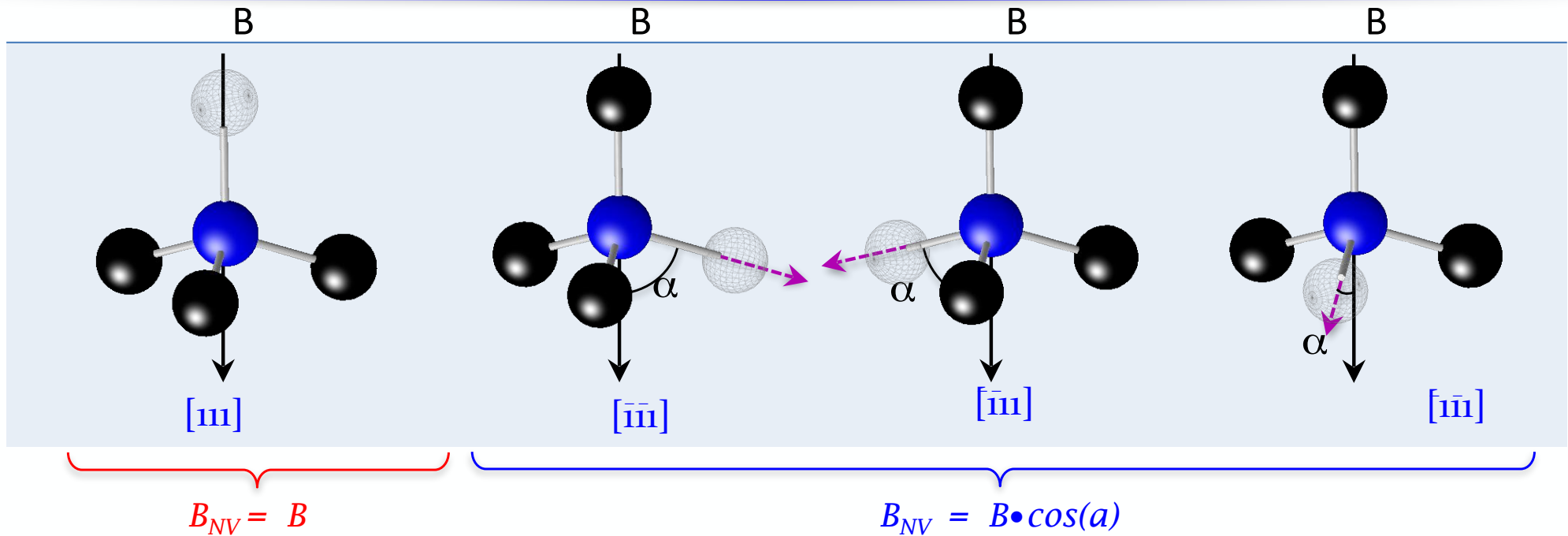
(111) – oriented diamond growth



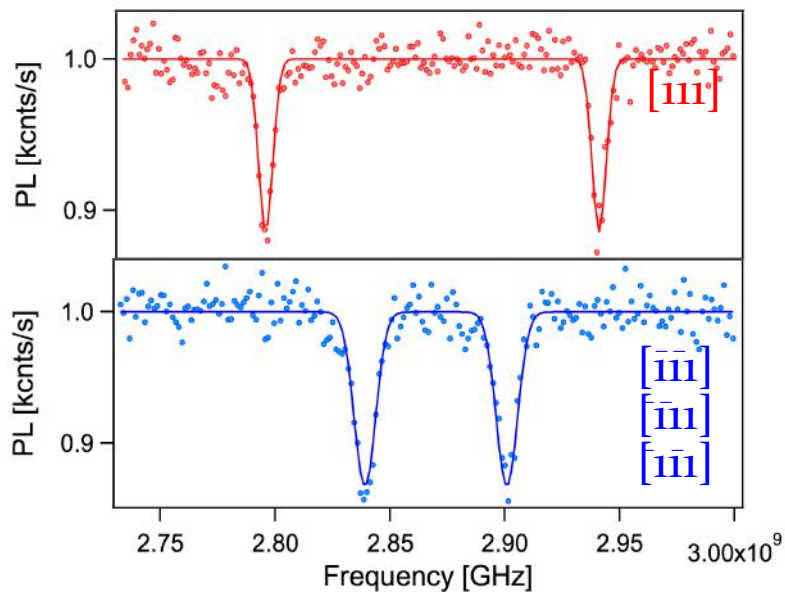
CVD diamond film
111 - grown
50 μm thick



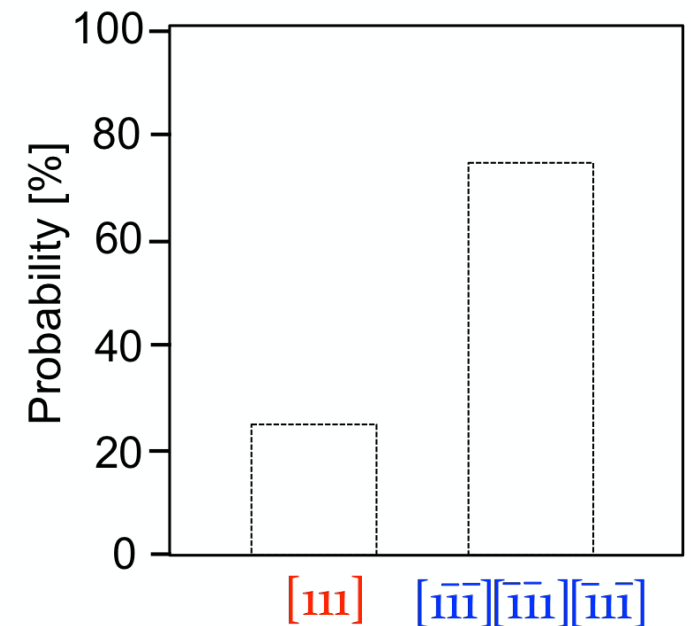
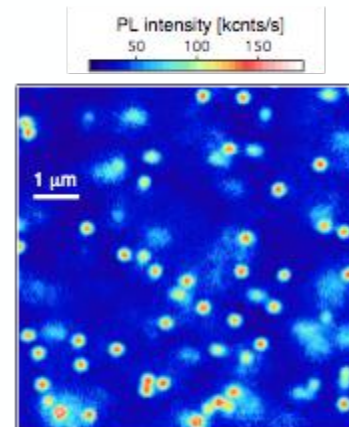
ESR shift measurement



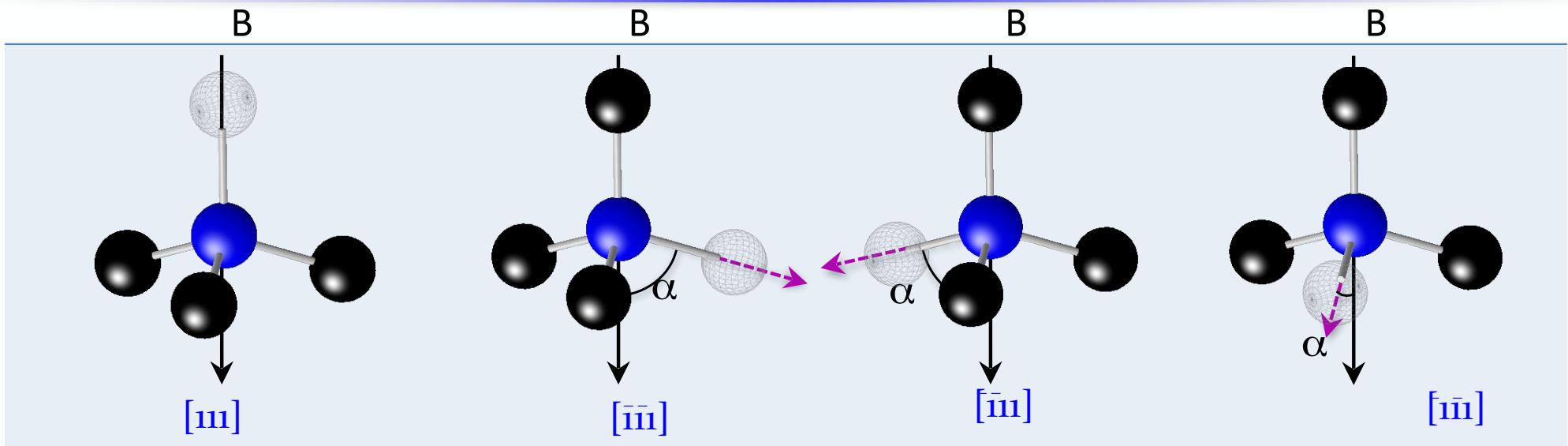
NV center orientation discrimination
by ESR shift measurements



Statistics on more
than 200 NVs



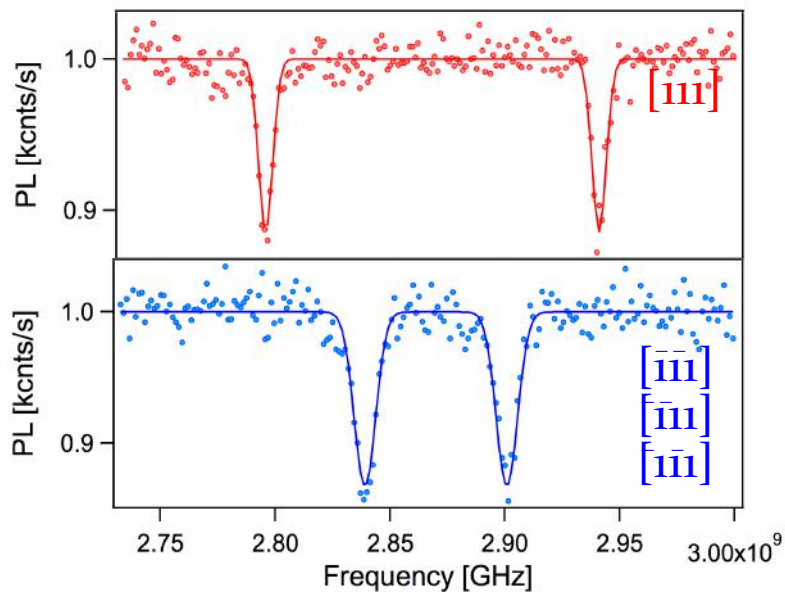
ESR shift measurement



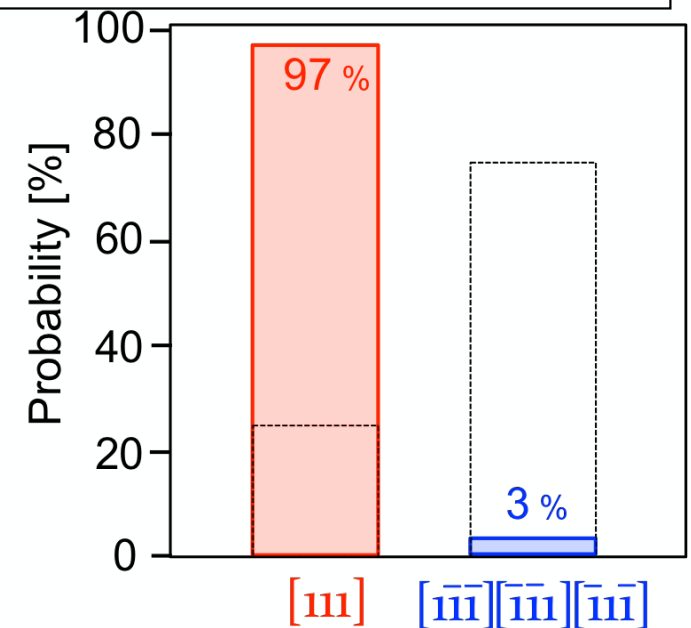
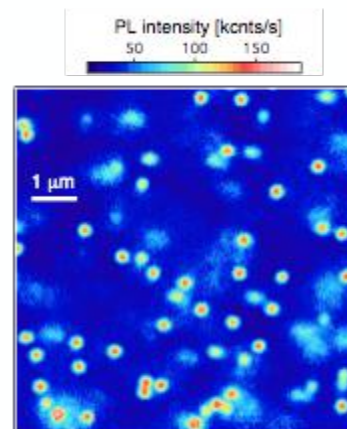
$$B_{NV} = B$$

NV center orientation discrimination
by ESR shift measurements

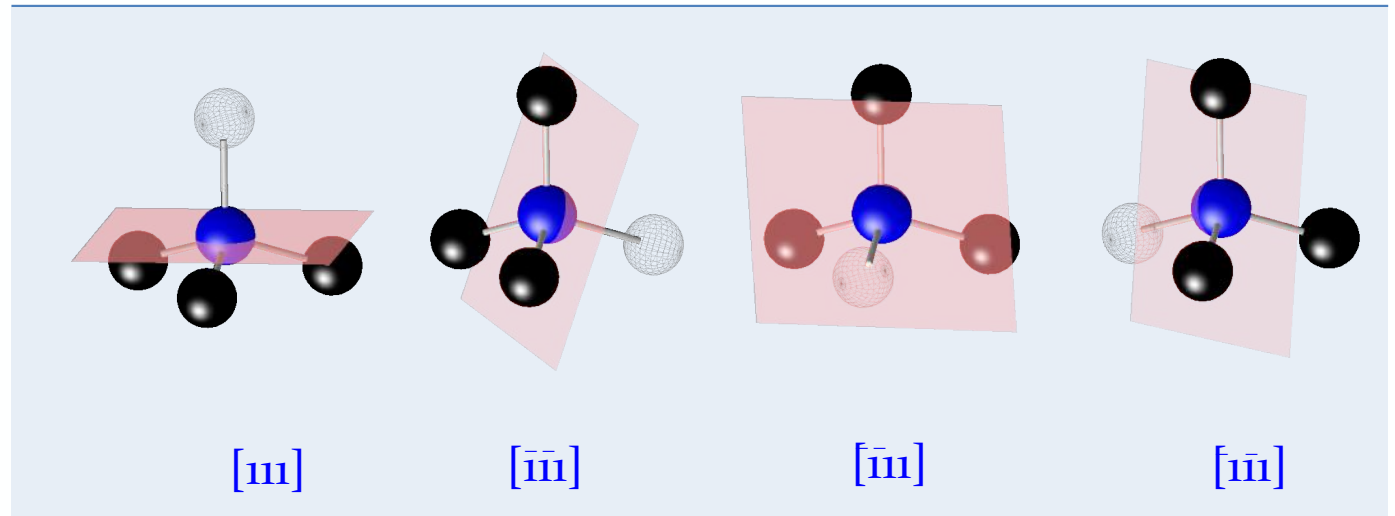
- * M. Lesik, et al., Appl. Phys. Lett., 104, 113107 (2014)
- ** J. Michl, et al., Appl. Phys. Lett., 104, 102407 (2014)
- *** T. Fukui, et al., Appl. Phys. Expr., 7, 055201 (2014)



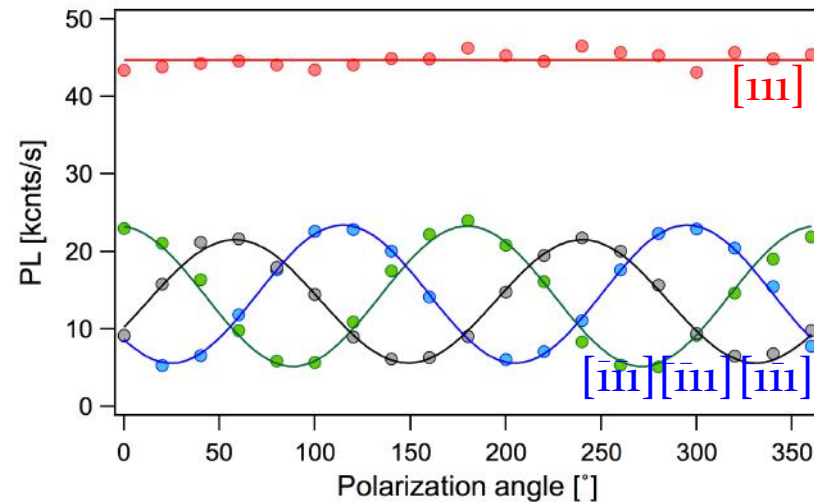
Statistics on more
than 200 NVs



Polarization dependent luminescence

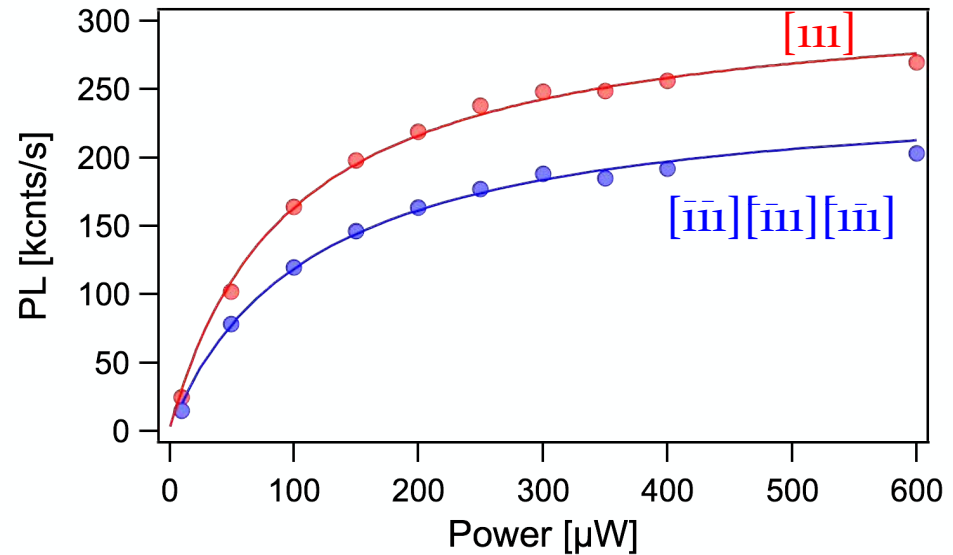
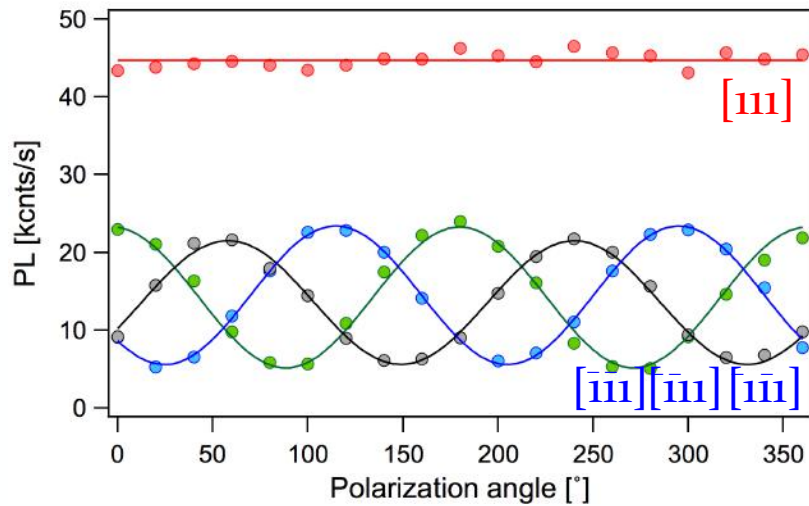


Polarization dependence



Polarization dependent PL can distinguish all 4 possible orientations

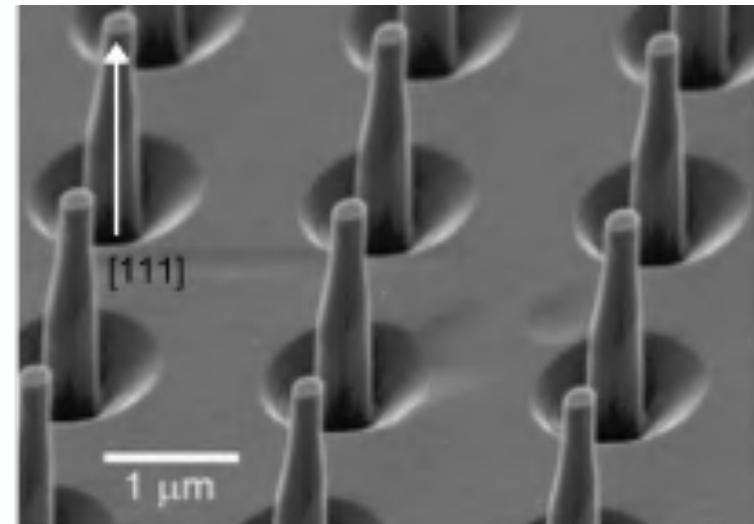
Orientation analysis (111)-oriented sample



Higher collection efficiency for 111-oriented NVs

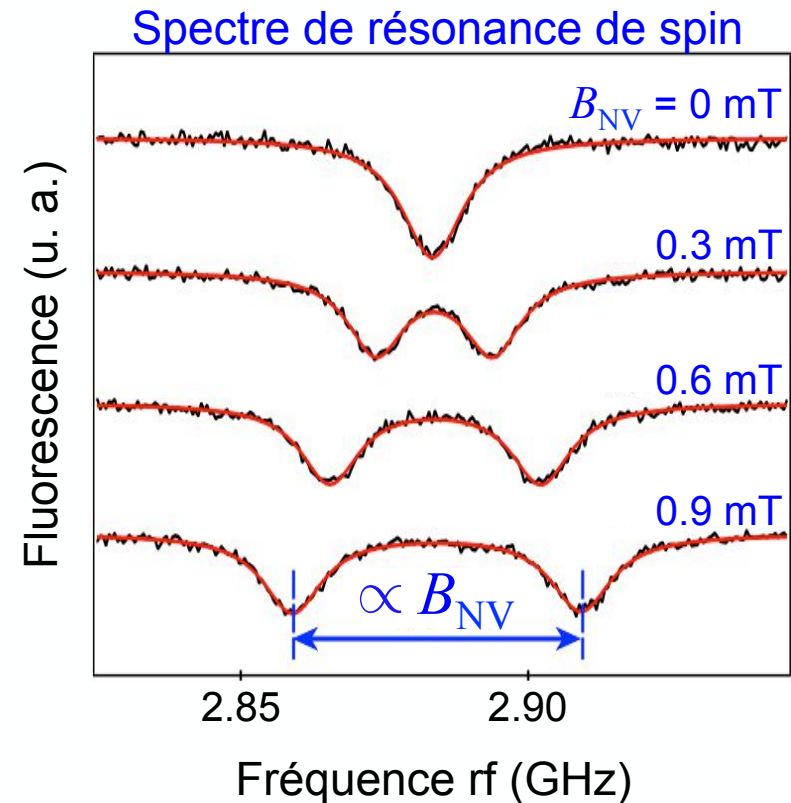
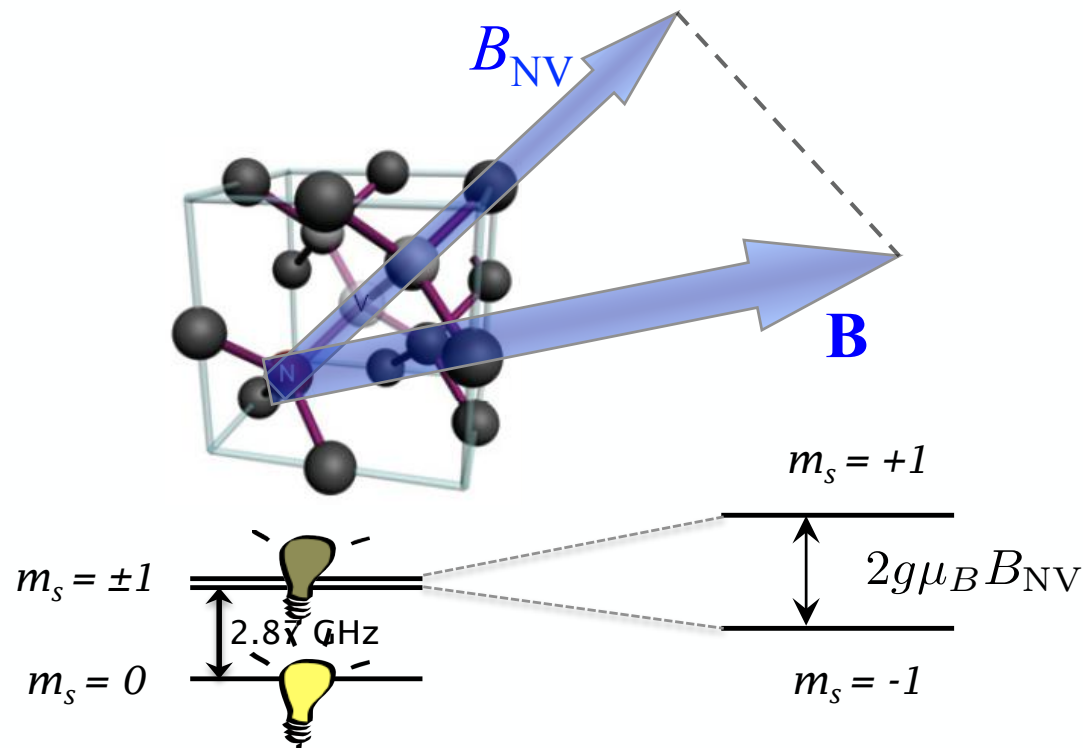
P. Maletinsky, University of Basel

Single NV center in a $[111]$ -oriented nanopillar
 PL signal of about 10^6 counts/s



* E. Neu, et al., Appl. Phys. Lett. 104, 153108 (2014)

The NV center in diamond: “Direct” magnetometry techniques

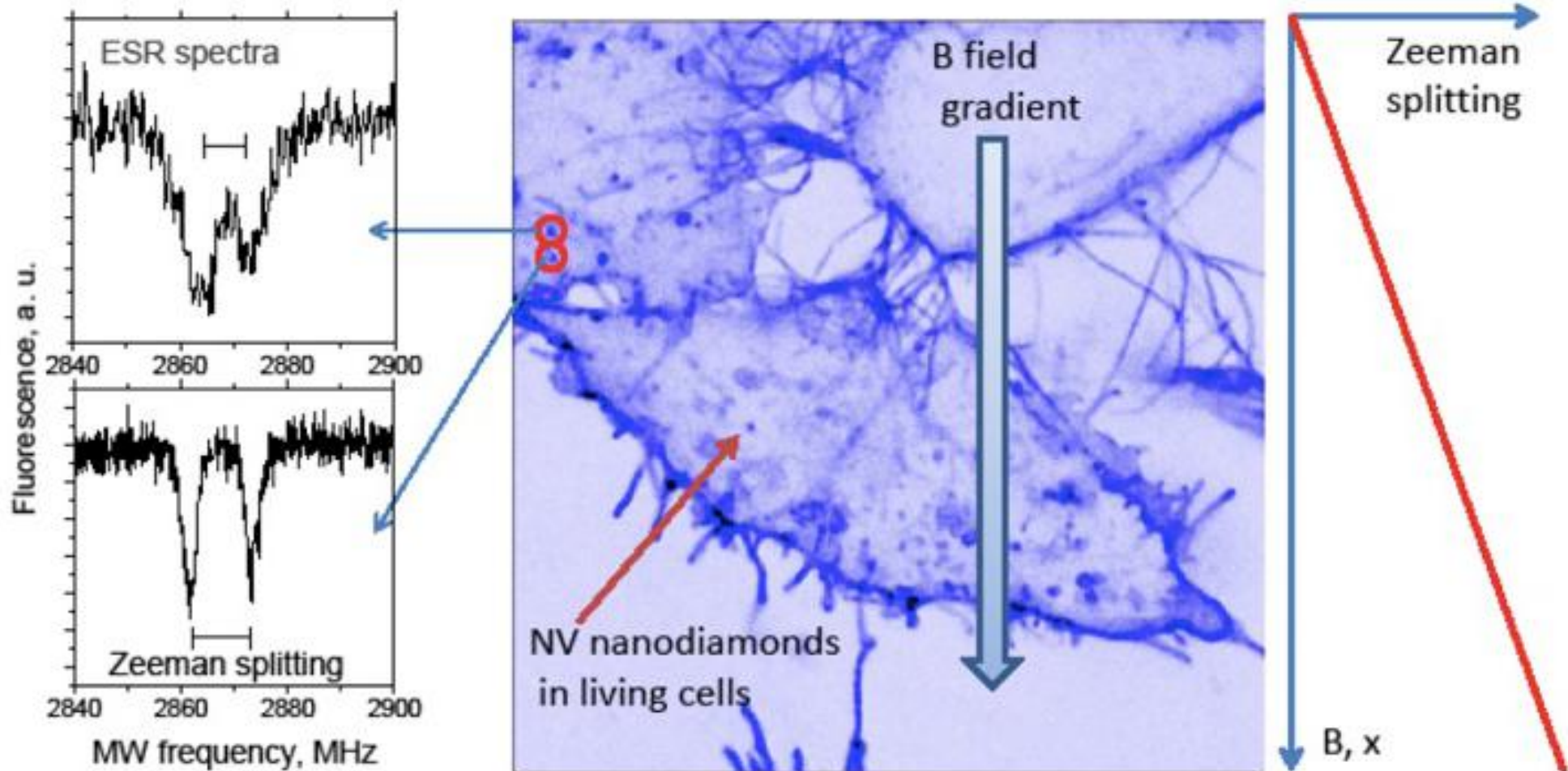


ODMR of NV centers in cells

Dynamics of Diamond Nanoparticles in Solution and Cells

Felix Neugart,[†] Andrea Zappe,[†] Fedor Jelezko,[†] C. Tietz,[†] Jean Paul Boudou,[‡] Anke Krueger,[§] and Jörg Wrachtrup^{*,†}

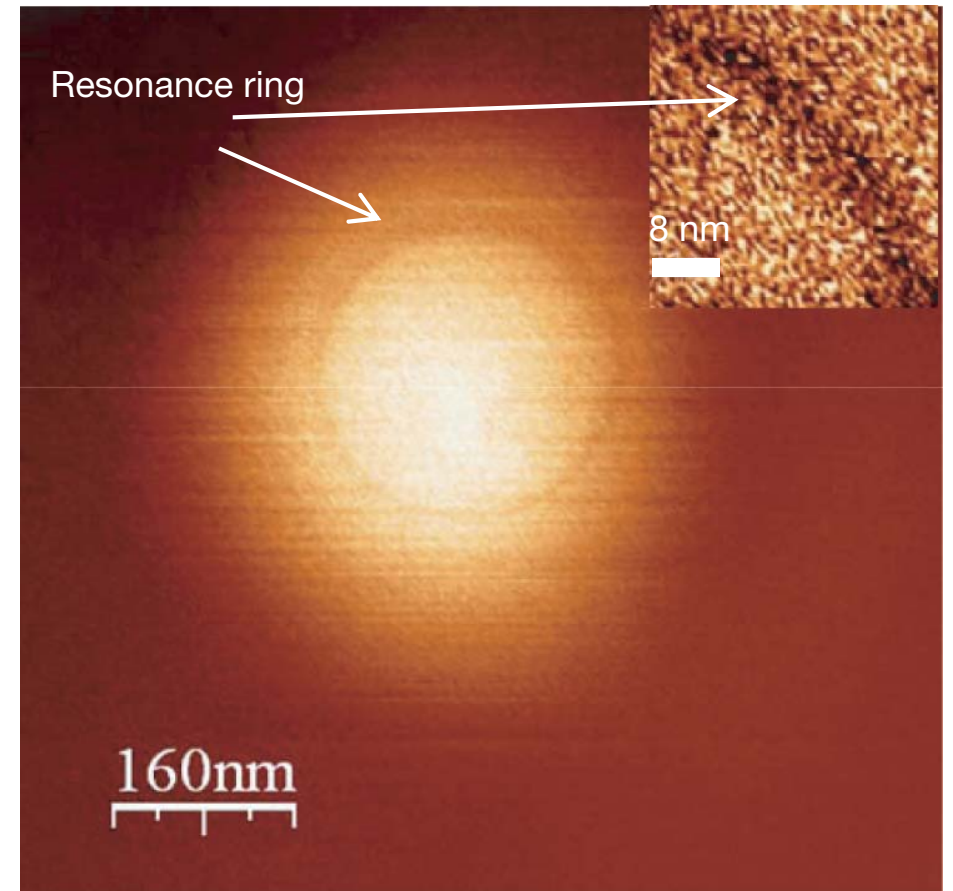
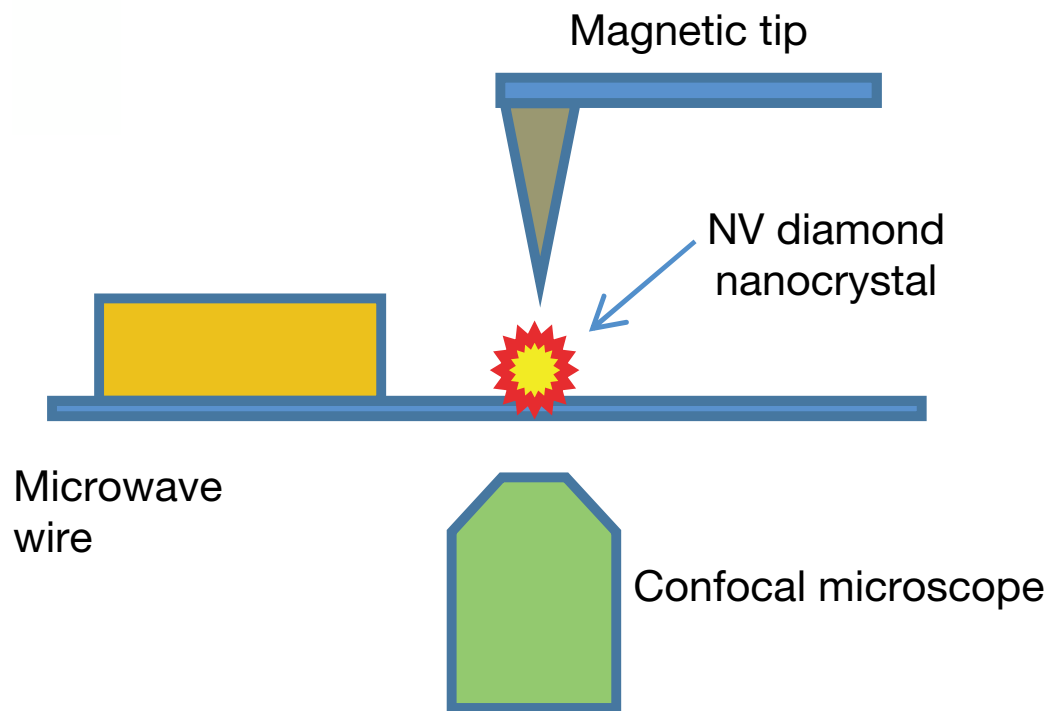
Nano Letters 7, 3588 (2007)



Nanoscale imaging magnetometry with diamond spins under ambient conditions

Nature 455, 648 (2008)

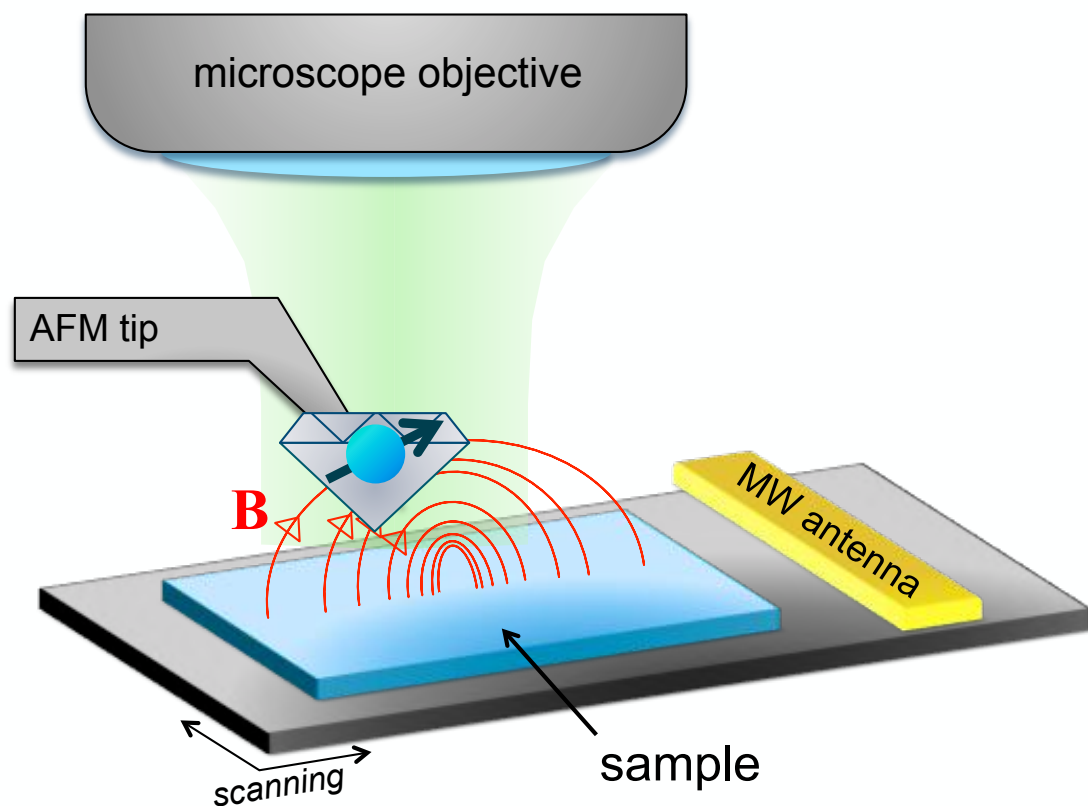
Gopalakrishnan Balasubramanian¹, I. Y. Chan²†, Roman Kolesov¹, Mohannad Al-Hmoud¹, Julia Tisler¹, Chang Shin³, Changdong Kim³, Aleksander Wojcik³, Philip R. Hemmer³, Anke Krueger⁴, Tobias Hanke⁵, Alfred Leitenstorfer⁵, Rudolf Bratschitsch⁵, Fedor Jelezko¹ & Jörg Wrachtrup¹



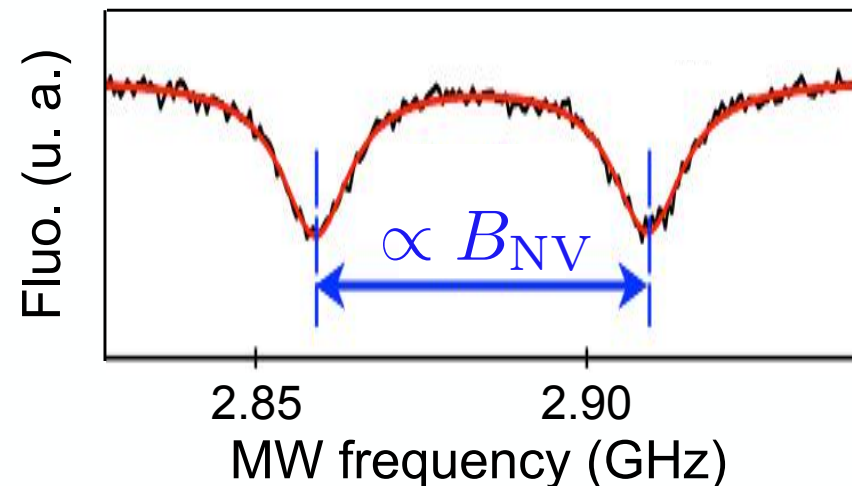
Field gradient $\approx 0.1 \text{ G/nm}$ at $1 \mu\text{m}$ distance of the tip
 $\Delta\nu_{\text{FWHM}} \approx 1 \text{ kHz} \rightarrow$ ultimate resolution $\approx 0.1 \text{ \AA}$

Magnetic probe based on a single NV spin

Proposal : B. M. Chernobrod & G. P. Berman,
J. Appl. Phys. 97, 014903 (2005)



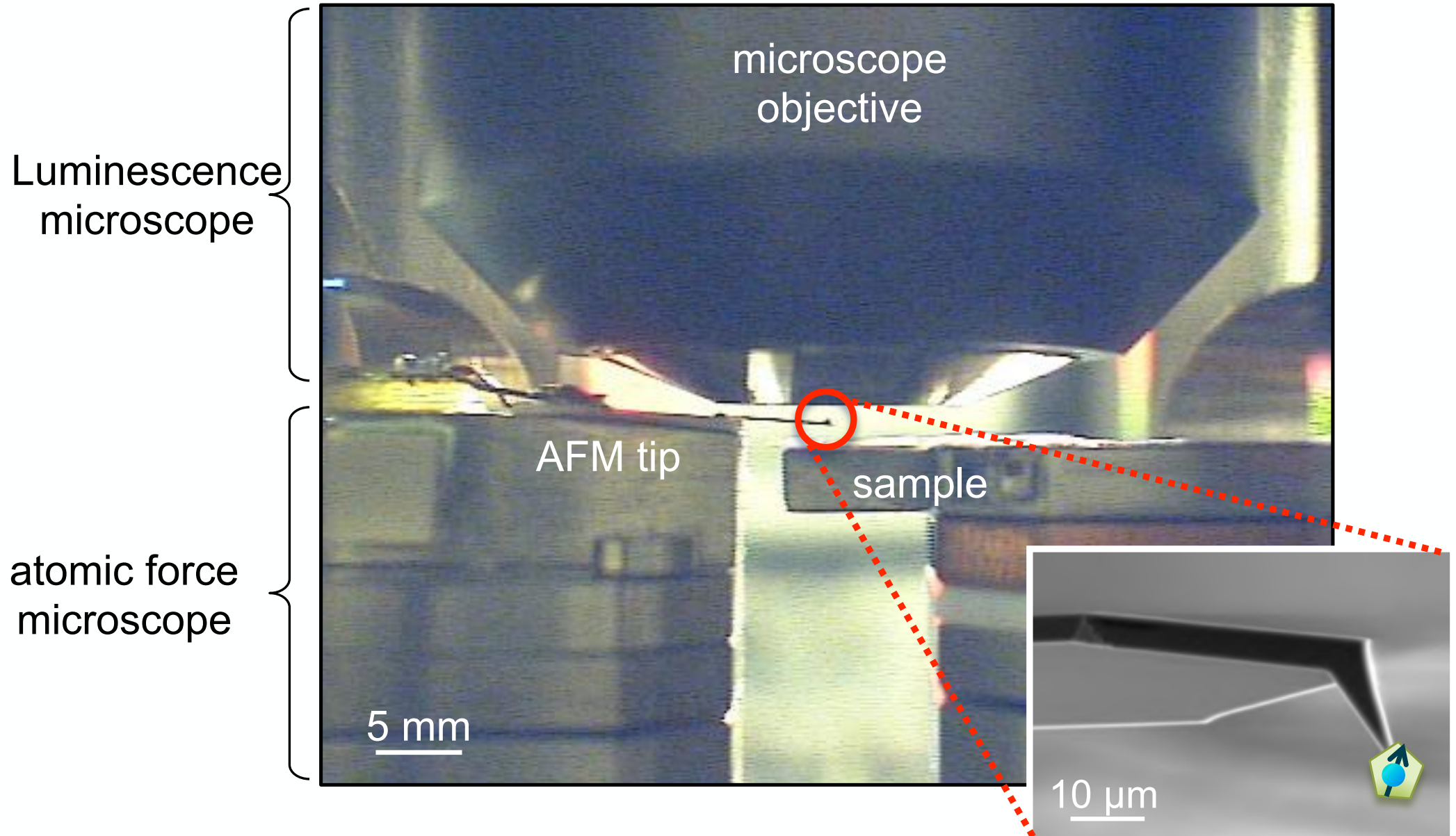
Spin resonance spectrum



- Quantitative measure of B_{NV} component
- Averaged over a volume $< (1 \text{ nm})^3$
- Ambient conditions without magnetic back-action (\neq MFM)

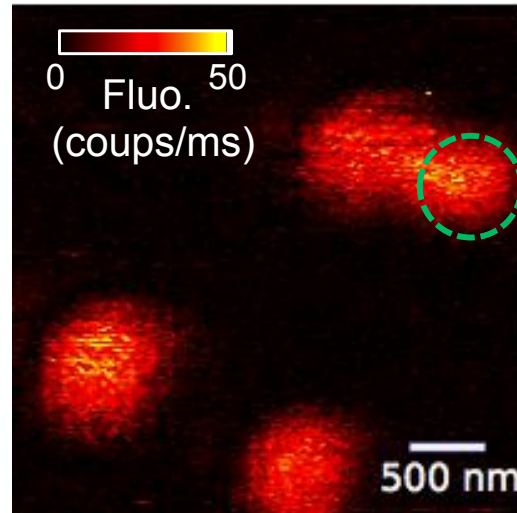
- First realization: G. Balasubramanian et al., Nature 455, 648 (2008)
- Review: L. Rondin et al., Rep. Prog. Phys. 77, 056503 (2014)

Practical implementation

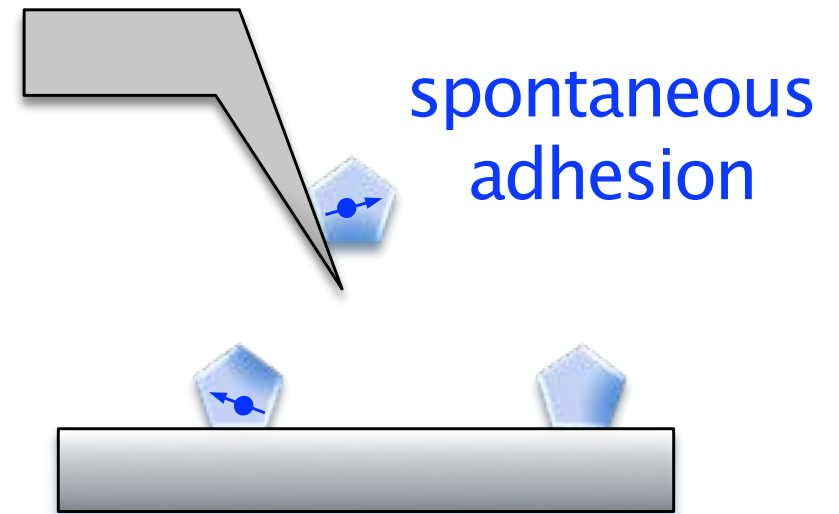
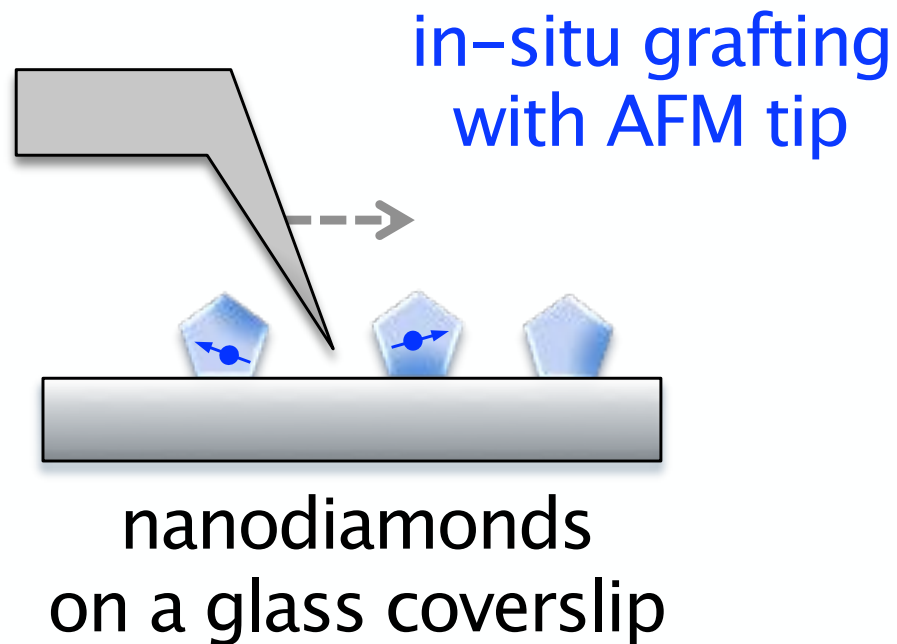
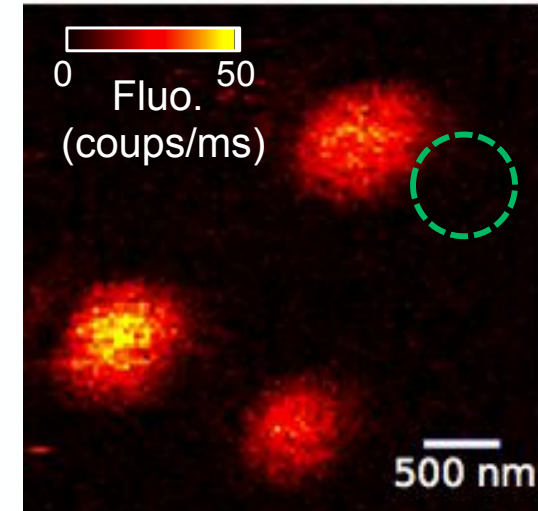


Grafting a nanodiamond on the AFM tip

before grafting

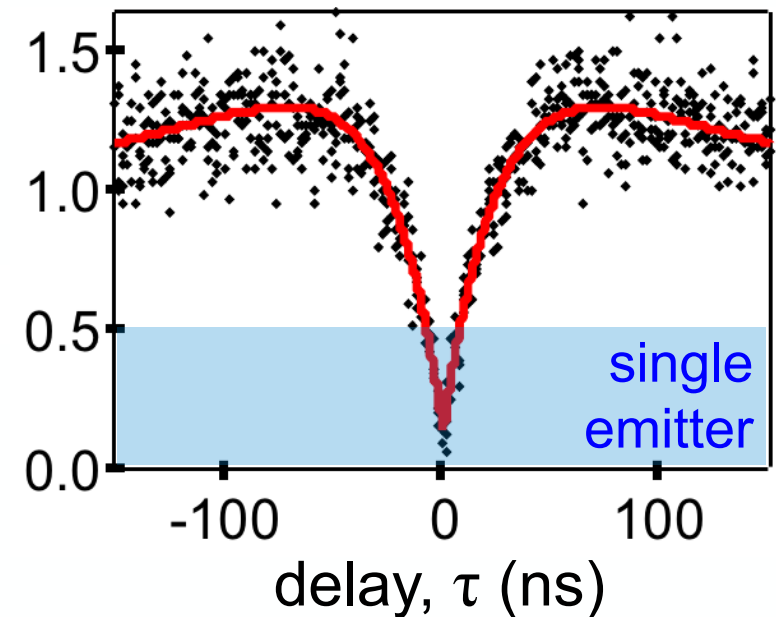
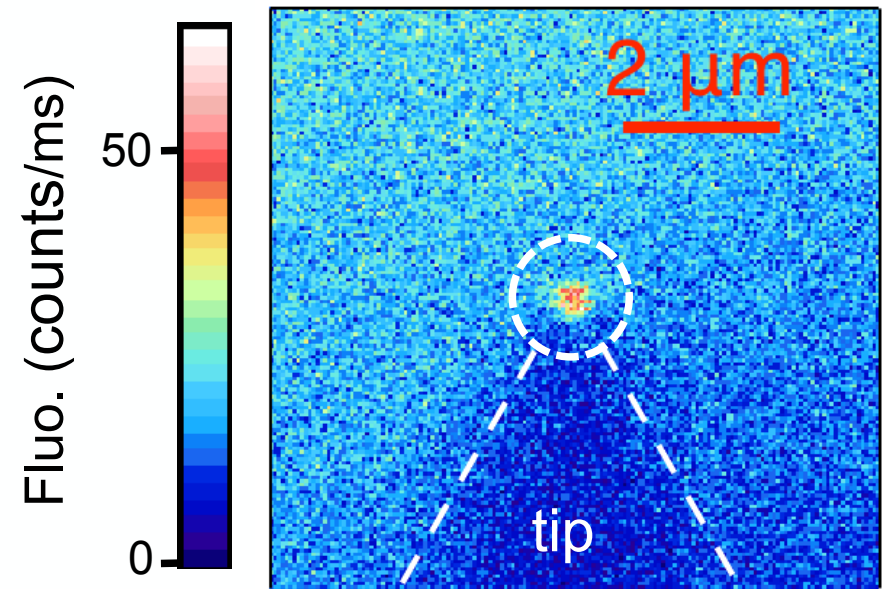
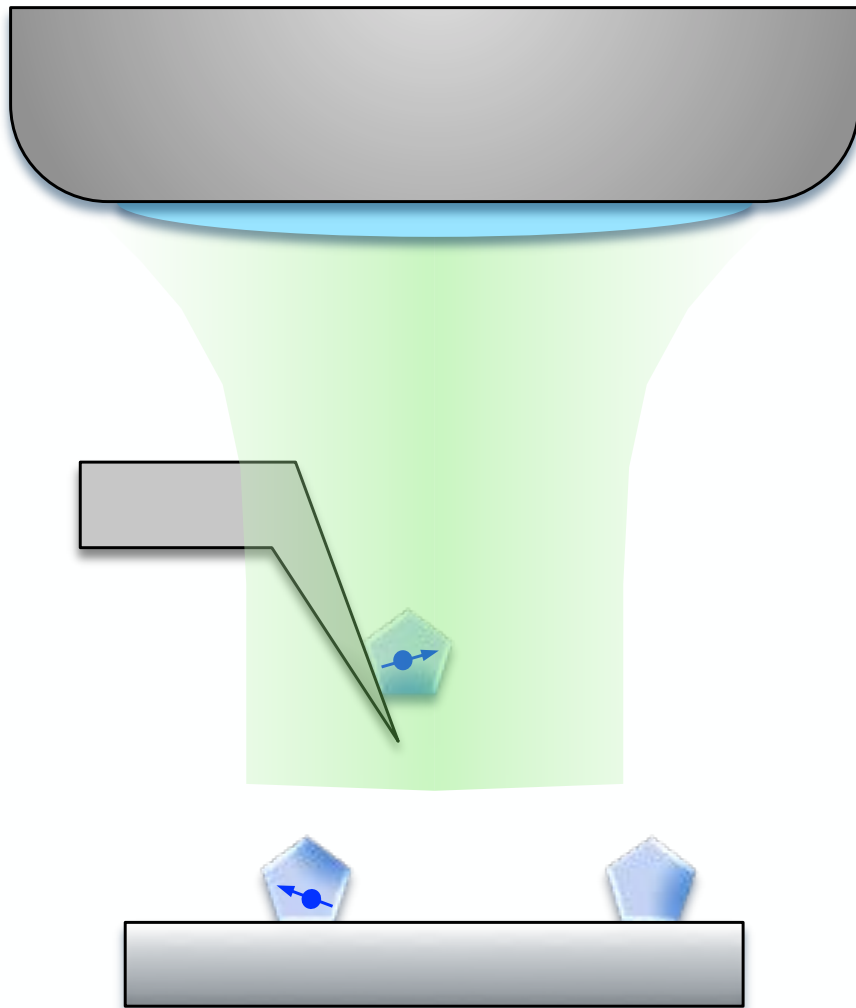


after grafting



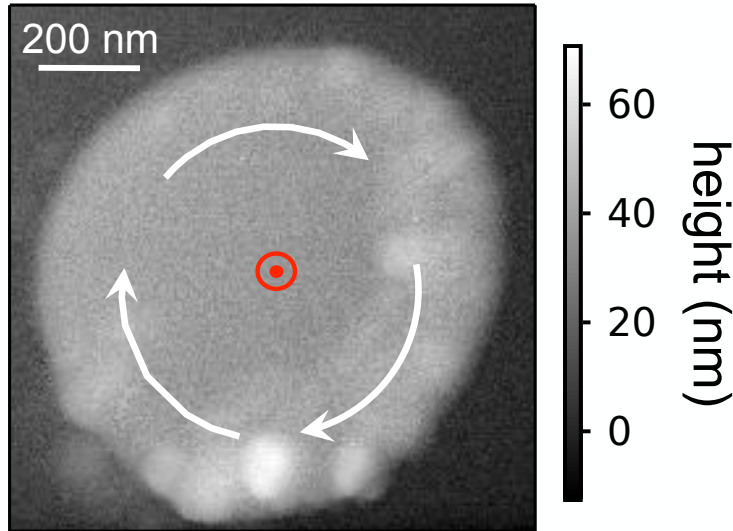
A single NV at the apex of the AFM tip

optical confocal microscope



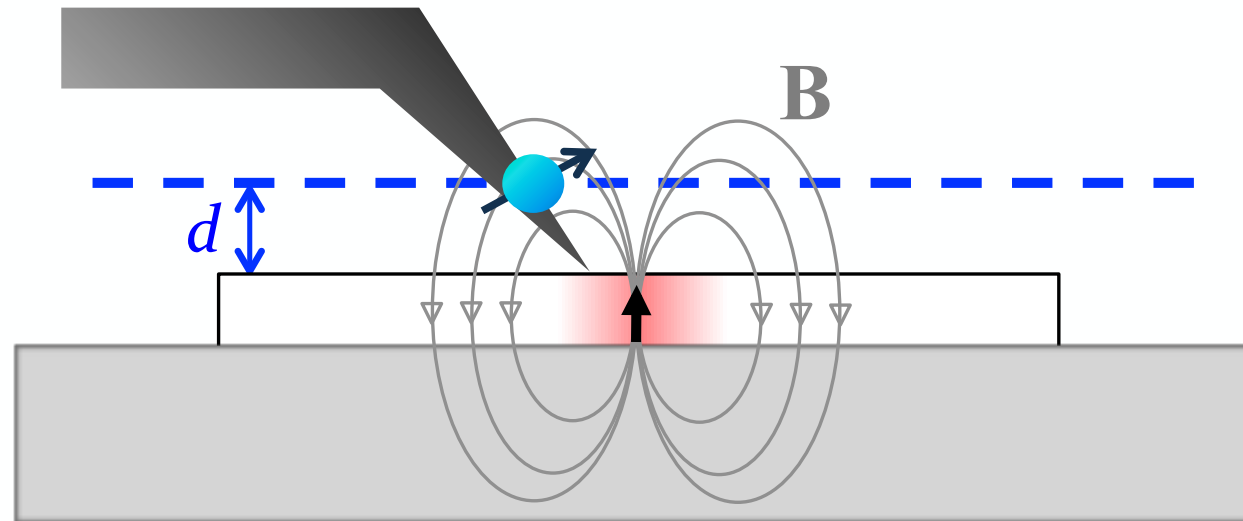
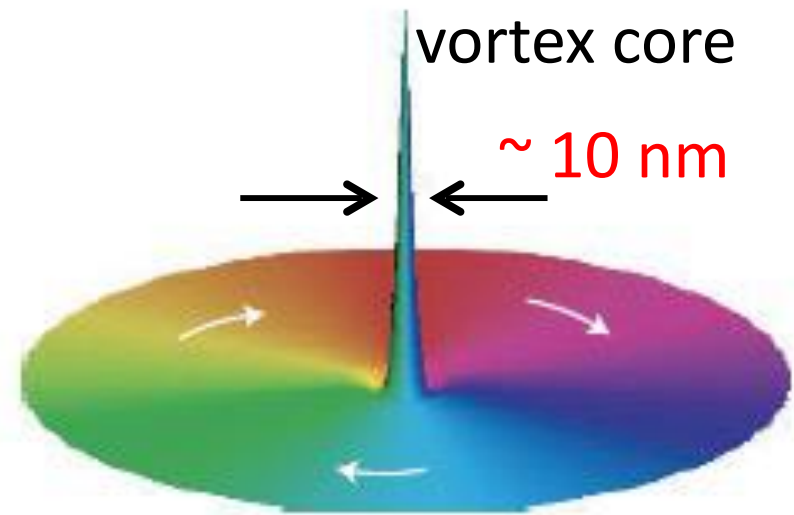
Proof-of-principle: core of magnetic vortex

AFM image

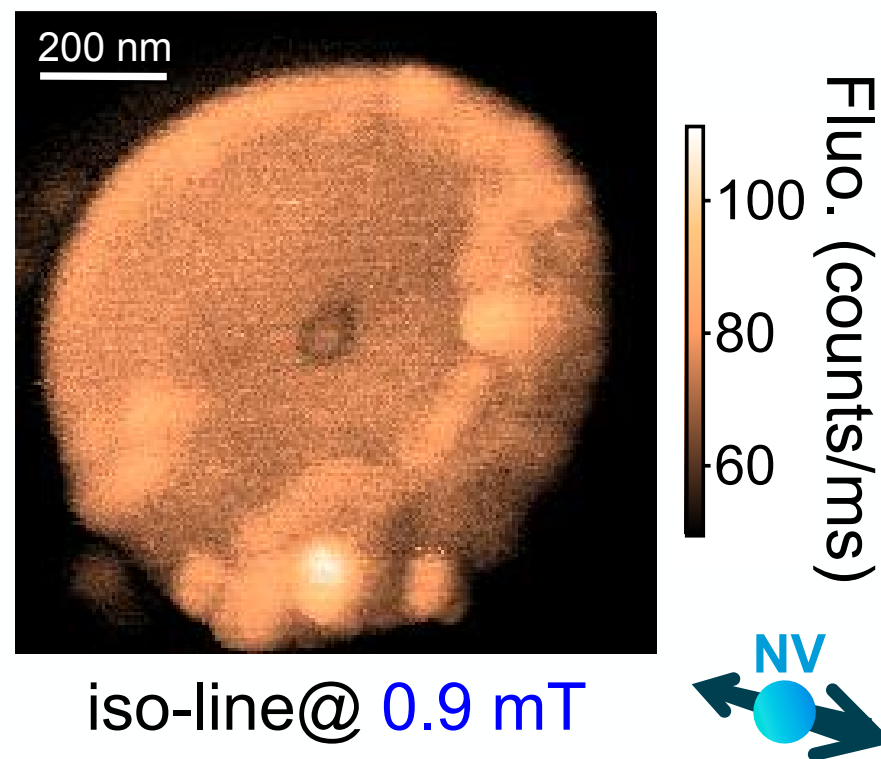
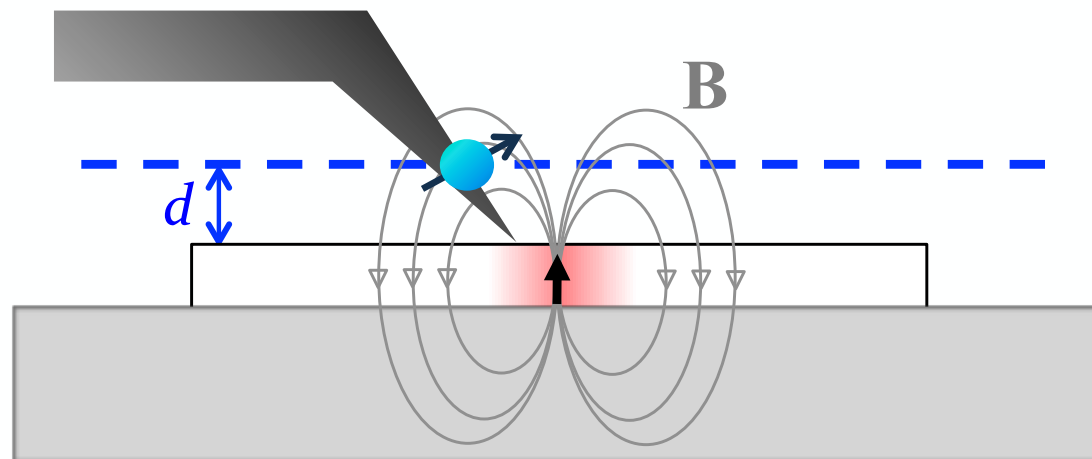
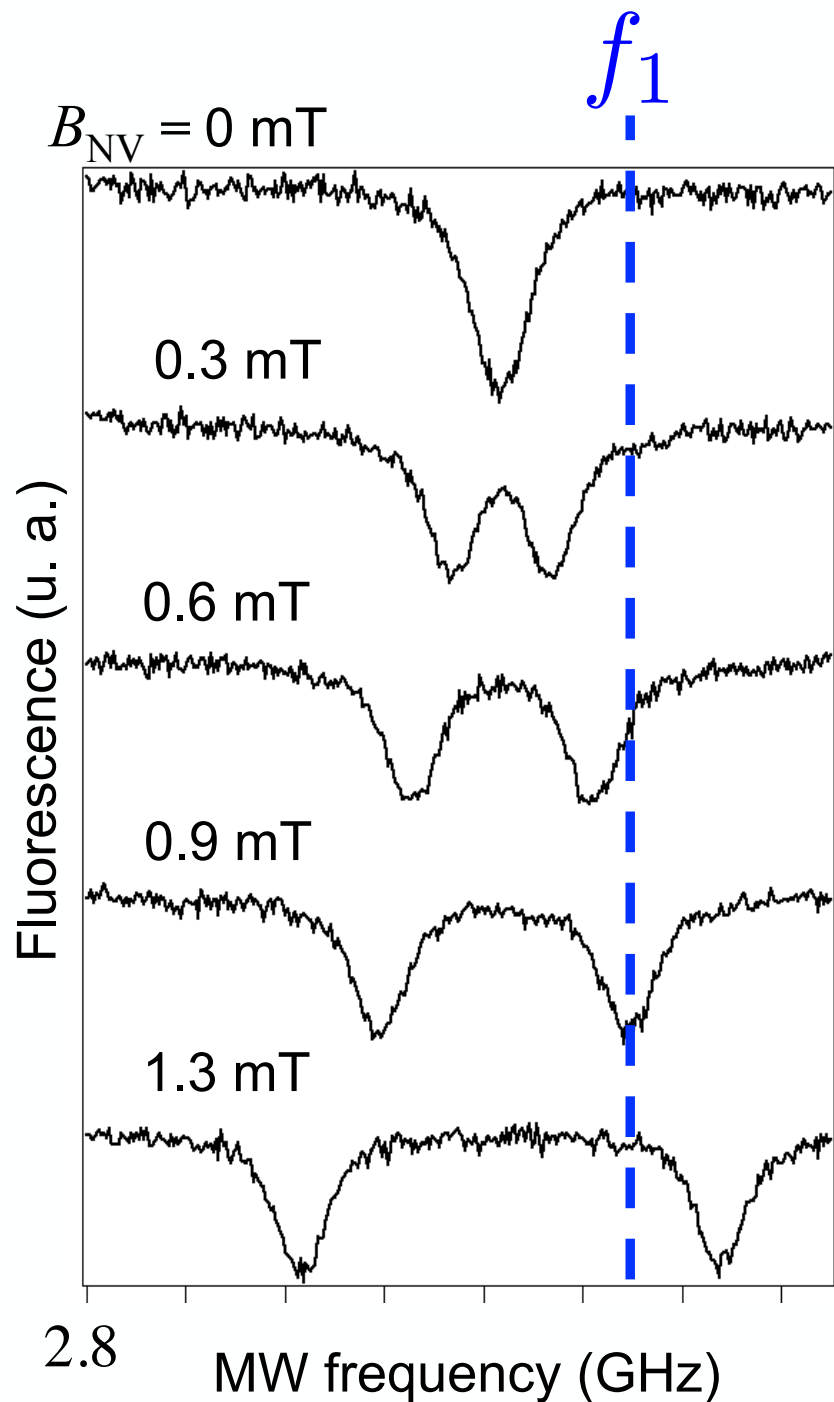


microdisk of $\text{Ni}_{80}\text{Fe}_{20}$

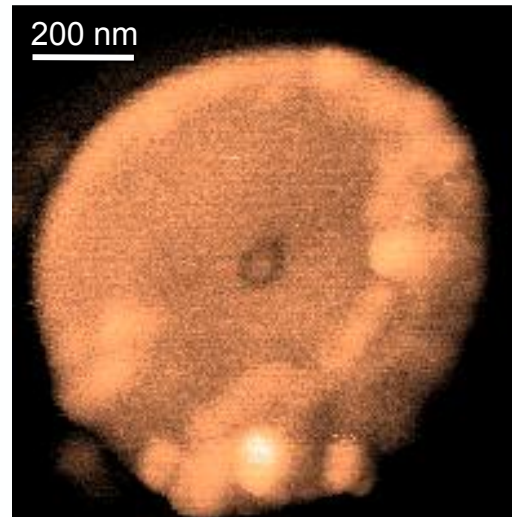
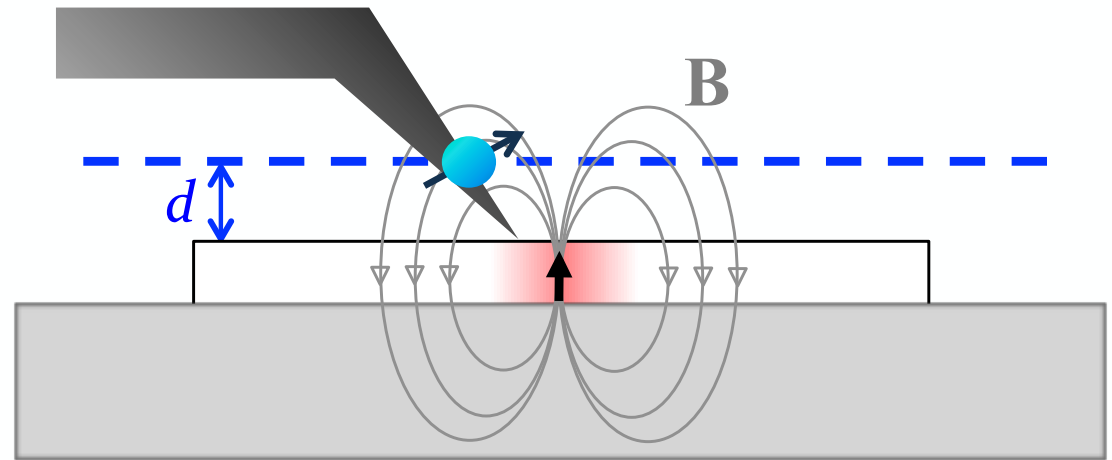
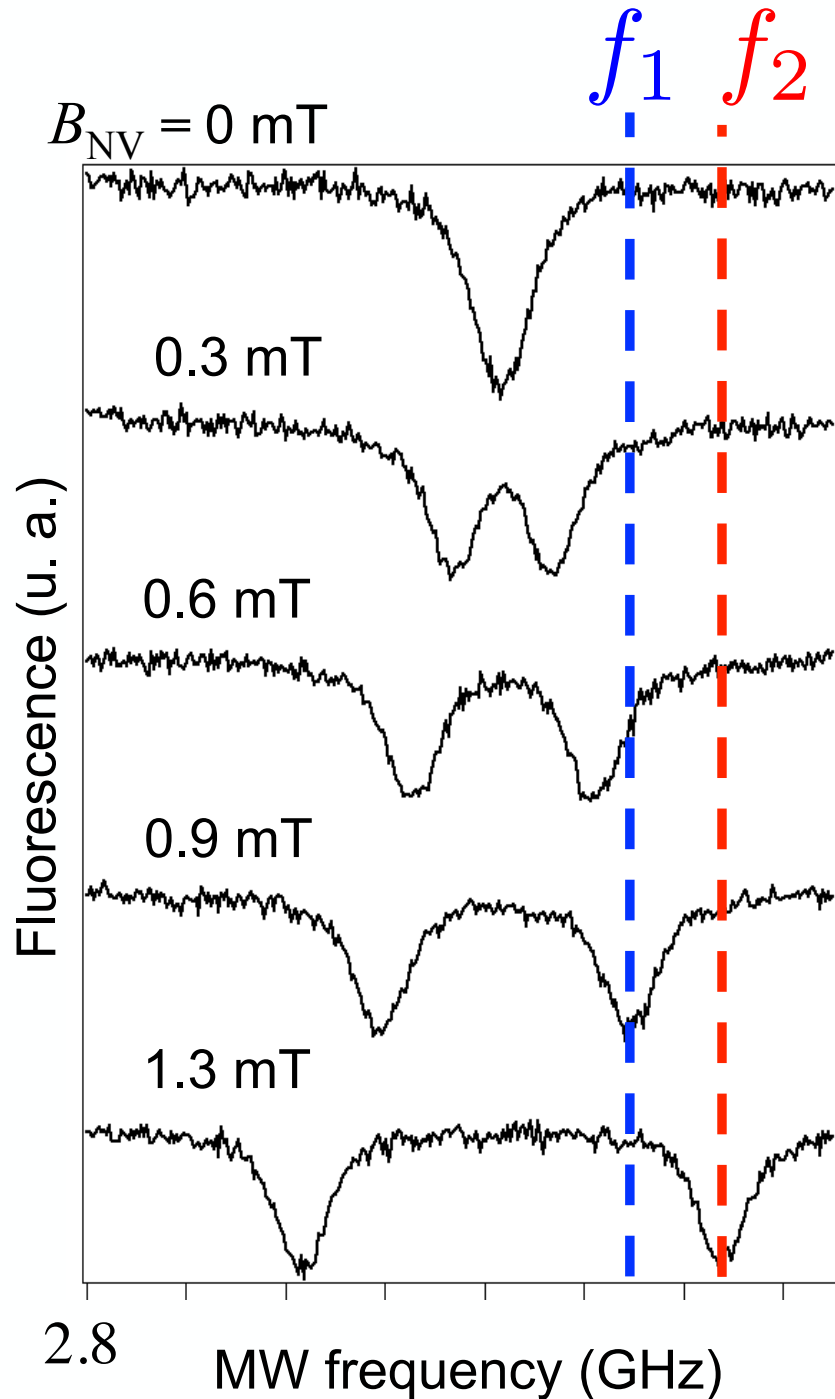
magnetization



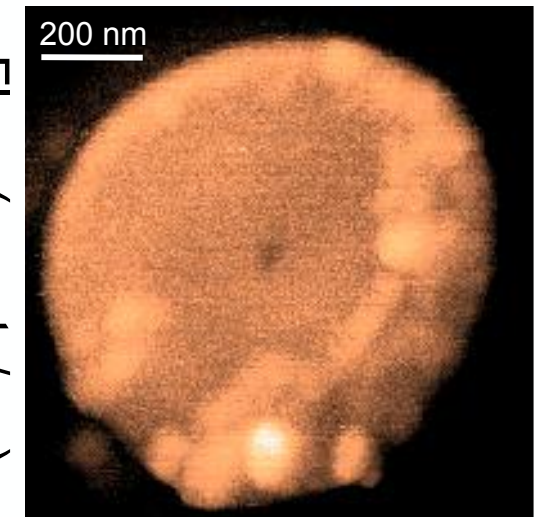
Magnetic imaging techniques (2)



Magnetic imaging techniques (3)



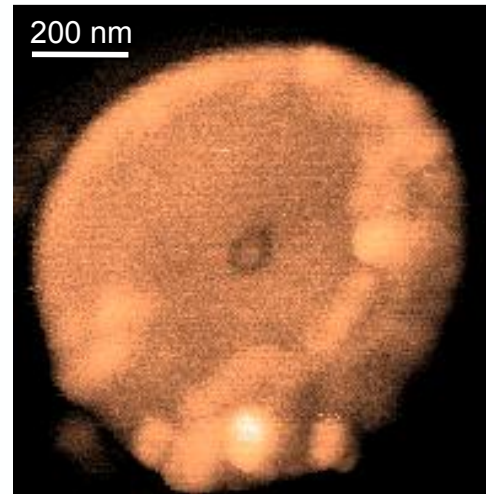
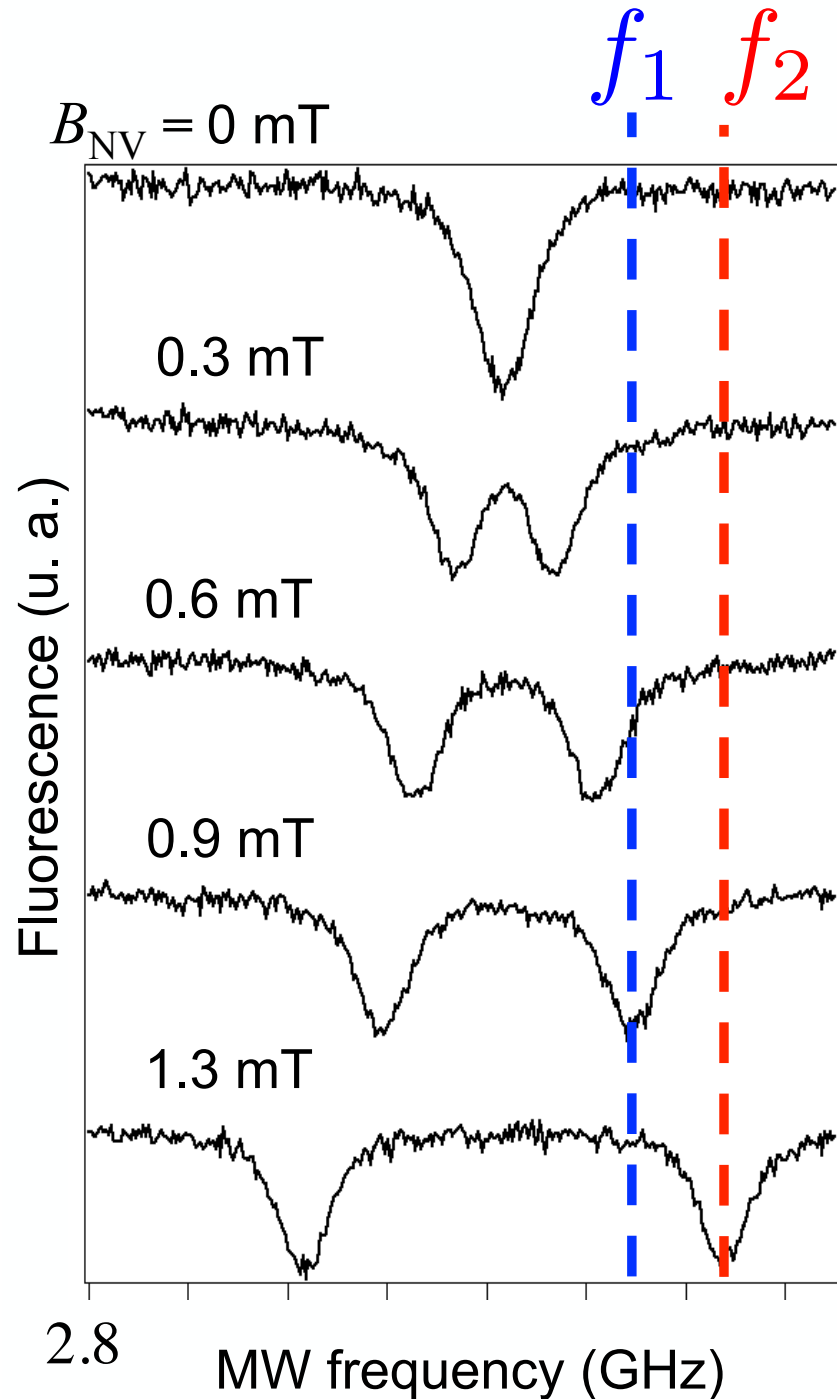
Iso-line @ 0.9 mT



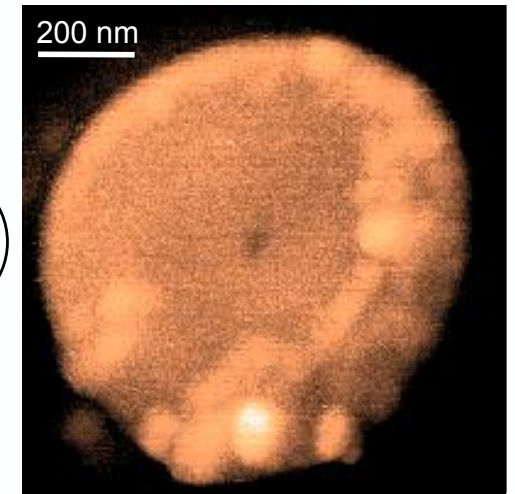
Iso-line @ 1.3 mT



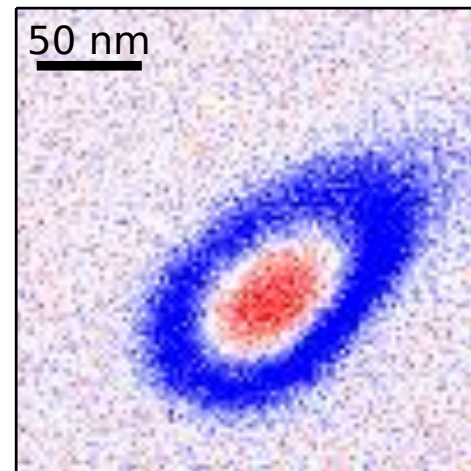
Magnetic imaging techniques (4)



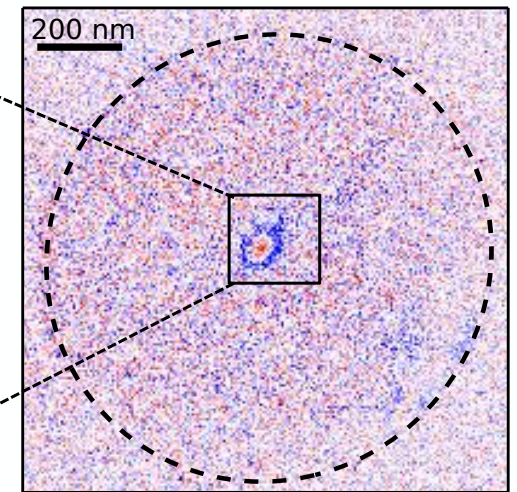
Iso-line @ 0.9 mT
Image



Iso-line @ 1.3 mT



$\sim 50 \text{ ms}$ per pixel



■ $B_{\text{NV}} = 1.3 \text{ mT}$
■ $B_{\text{NV}} = 0.9 \text{ mT}$

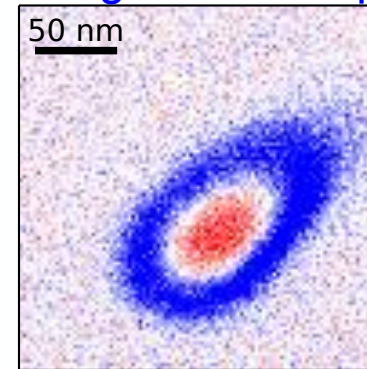
NV magnetometry

- Images of a vortex core

Rondin et al., Nature Communications 4, 2279 (2013).

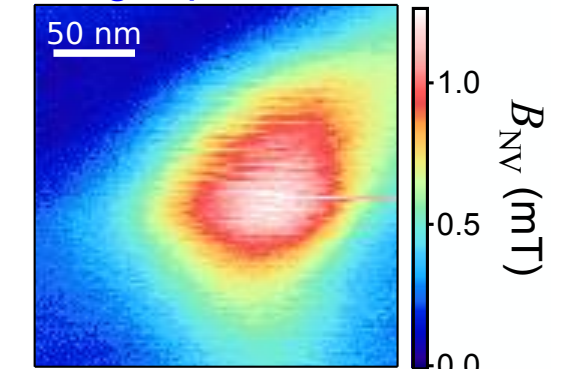
Tetienne et al., Phys. Rev. B 88, 214408 (2013).

Image iso-champ



~ 50 ms par pixel

Image quantitative



~ 500 ms par pixel

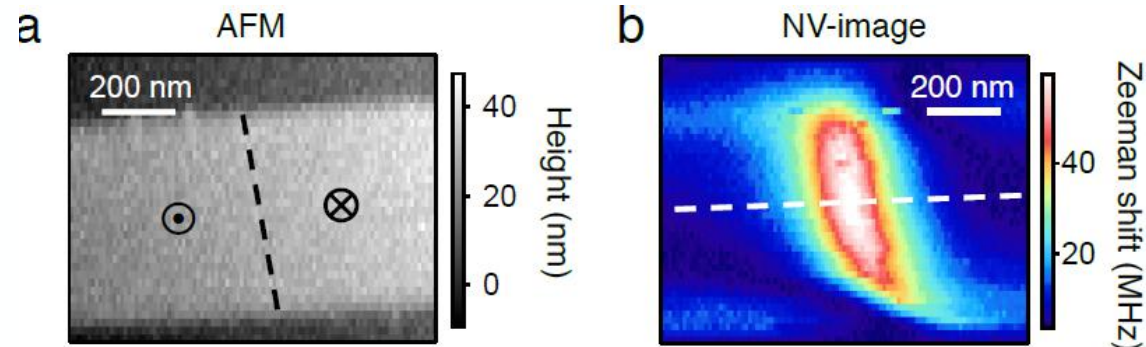
- Technique well suited for **quantitative** measurements on magnetic systems with nanoscale dimension

- Domain wall motion in a magnetic wire and Barkhausen noise

Tetienne, Hingant et al., Science 344, 6190 (2014)

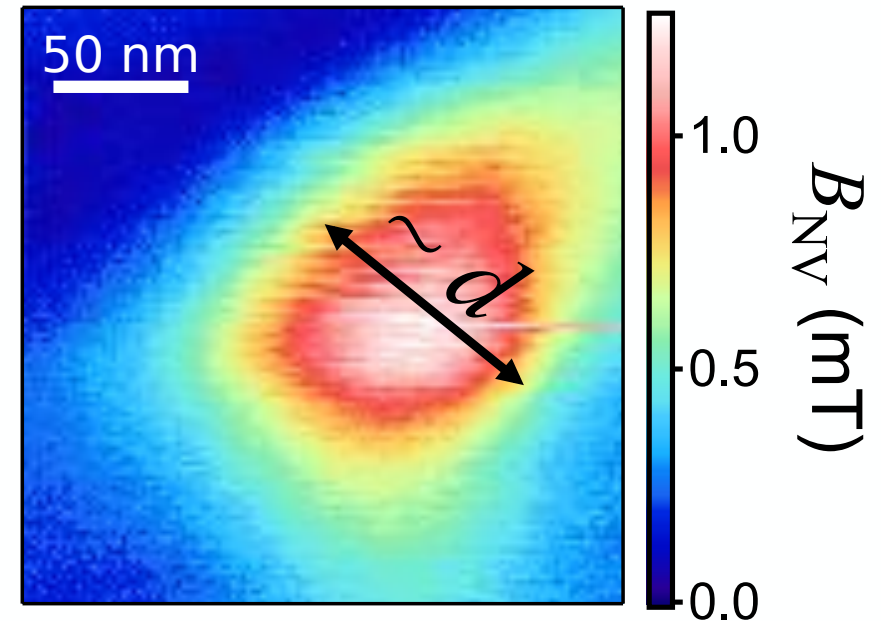
- Determine the structure of a single domain wall: Bloch or Néel

Tetienne, Hingant, et al., Nature Com. 6, 6733 (2015)

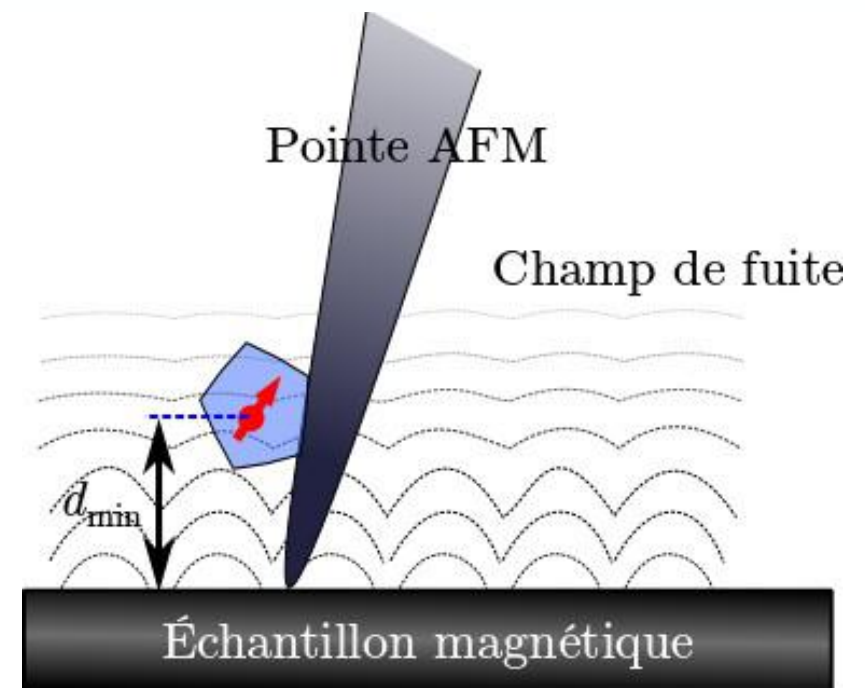
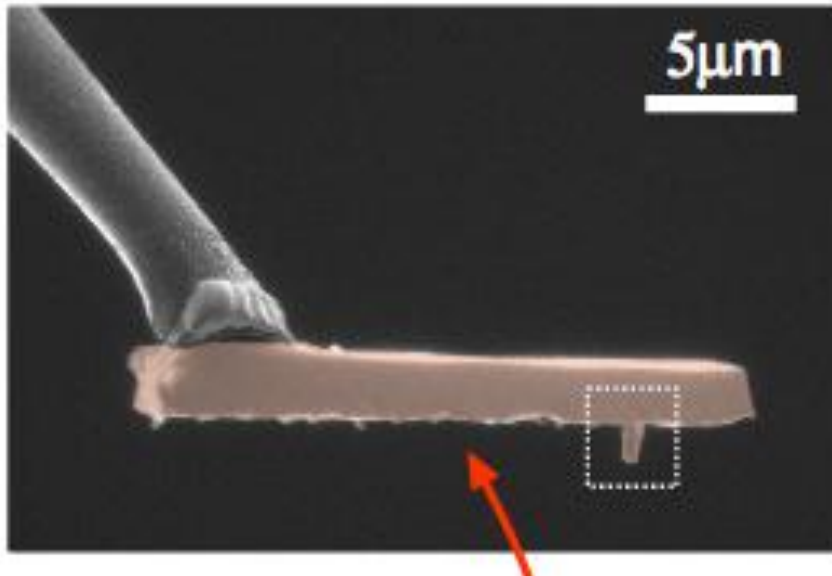


Resolution and magnetic sensitivity

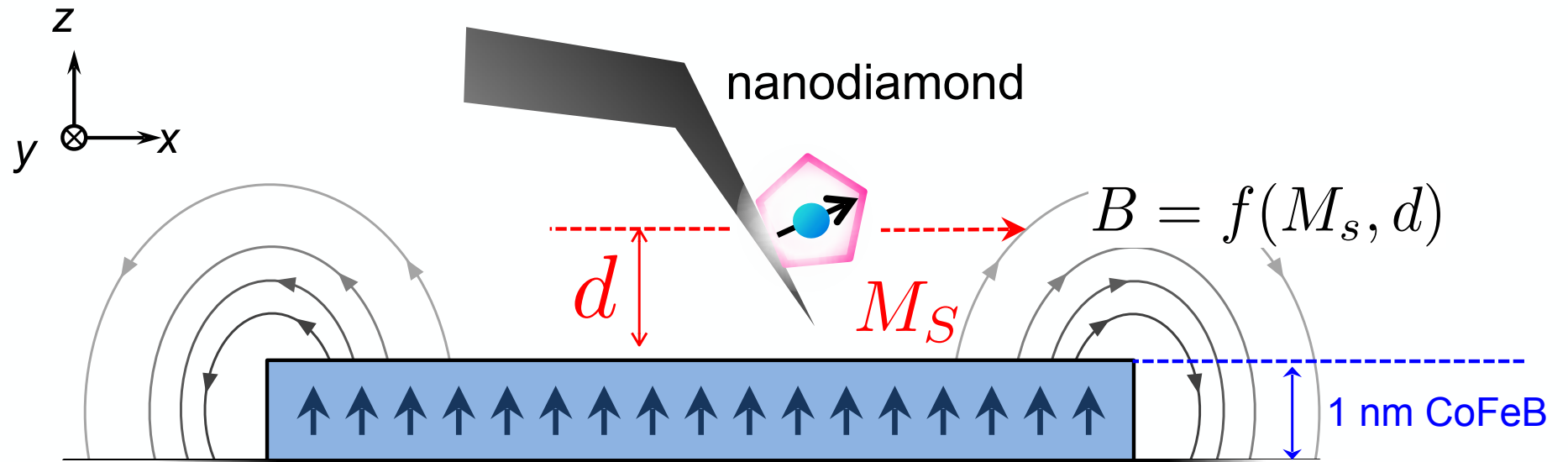
- Resolving power limited by “height of flight” (50 à 100 nm)
- B-field detected on a sampling volume of $\sim(1 \text{ nm})^3$
- Sensitivity limited by:
 - coherence time of NV spin
 - photon collection efficiency



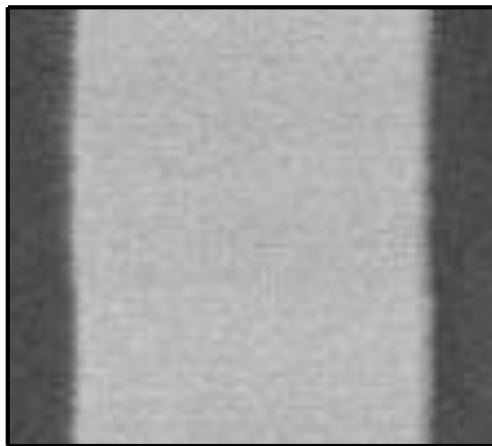
Improvement: diamond tip



Calibration of probe-to-sample distance

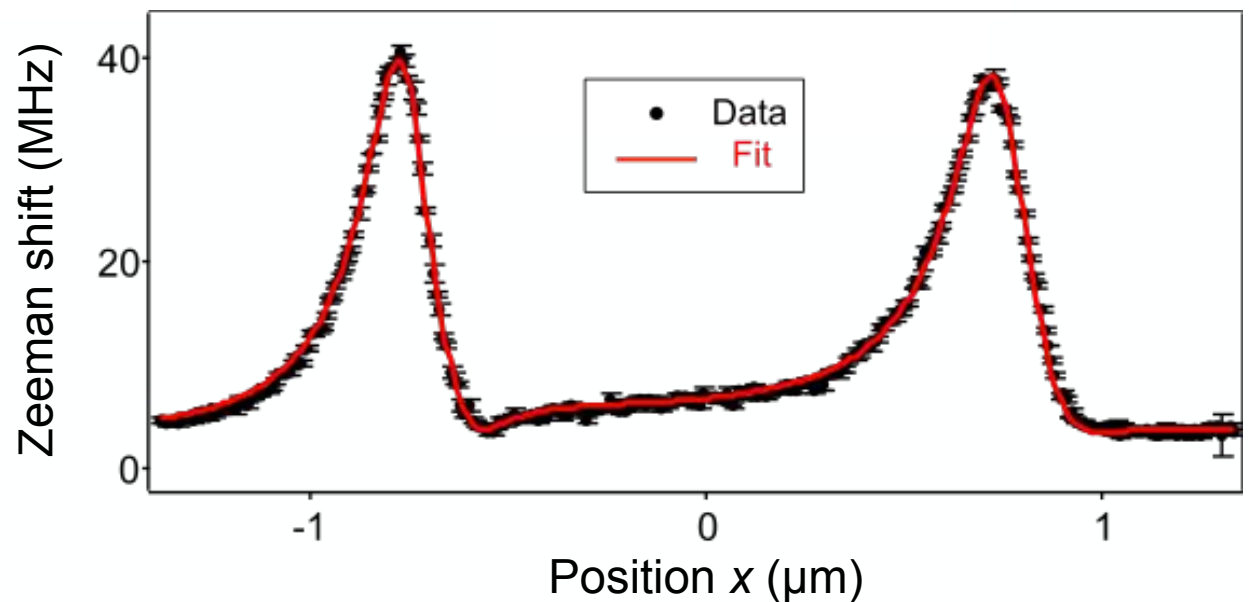


AFM image

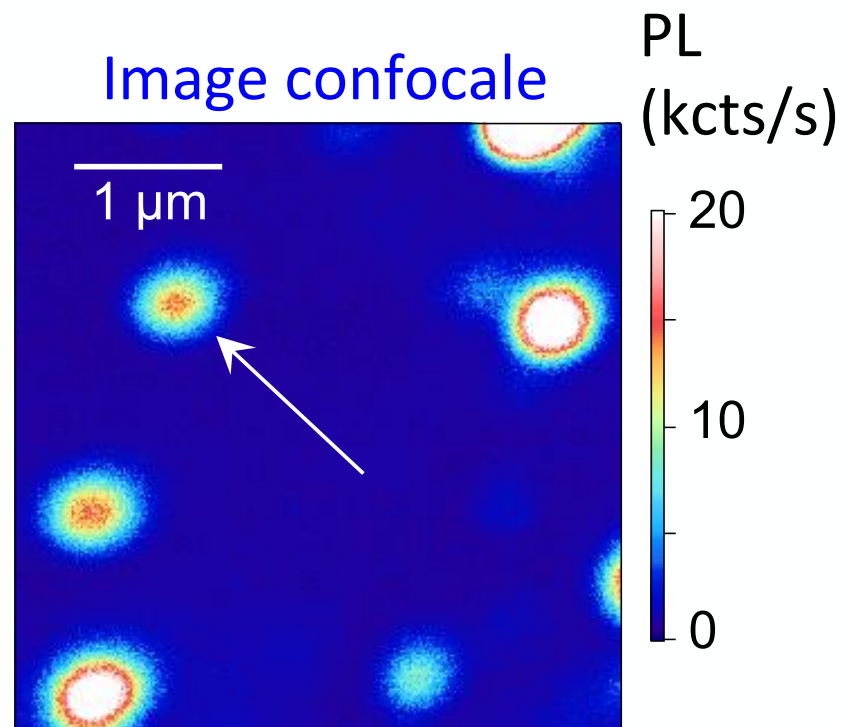
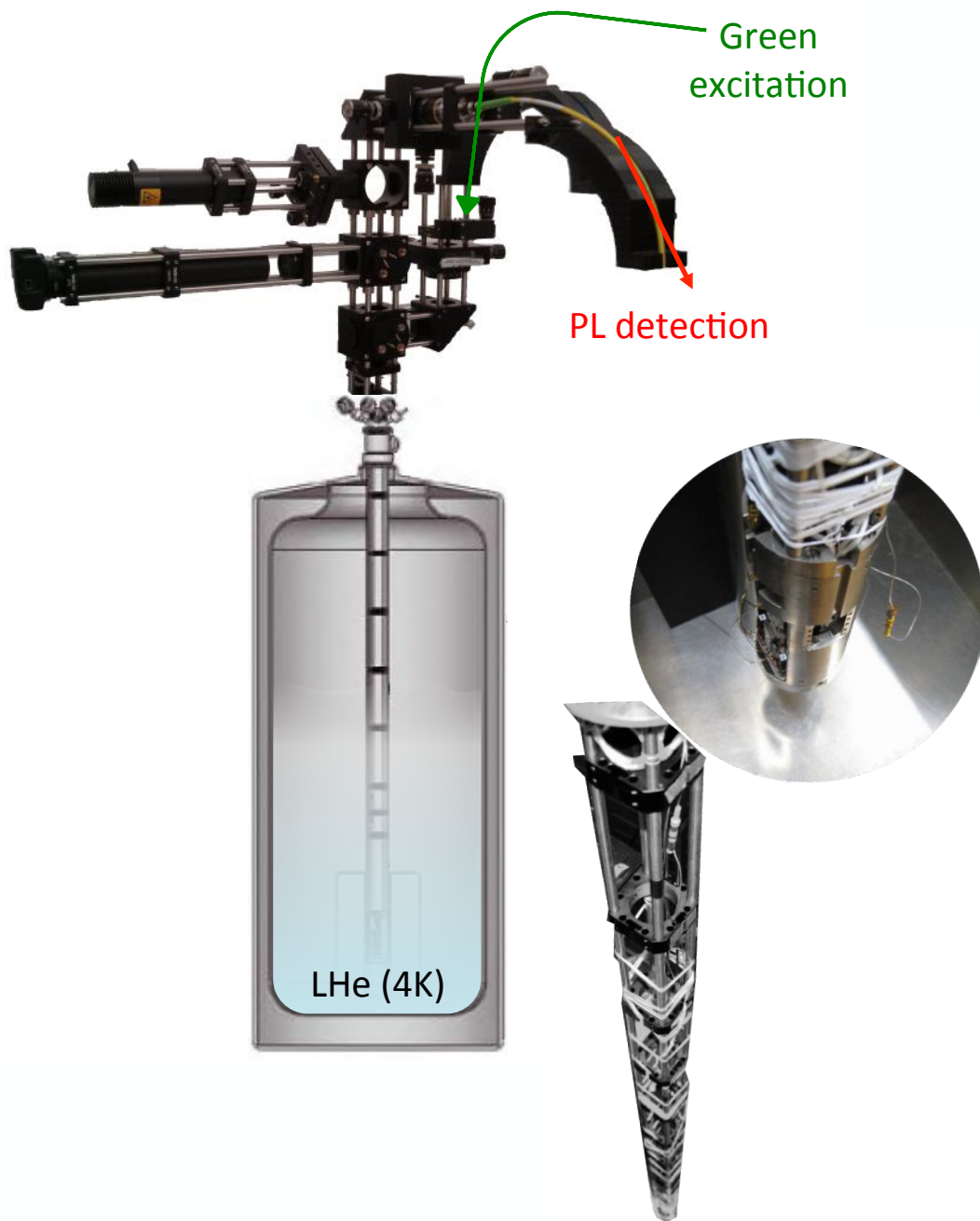


$$M_s = 0.93 \pm 0.03 \text{ MA/m}$$

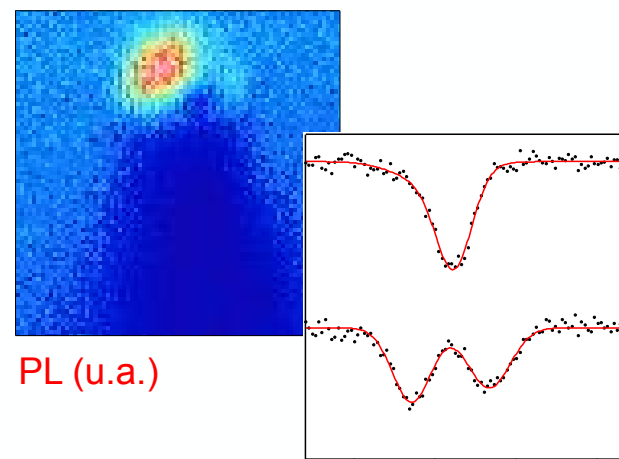
$$d = 123 \pm 3 \text{ nm}$$



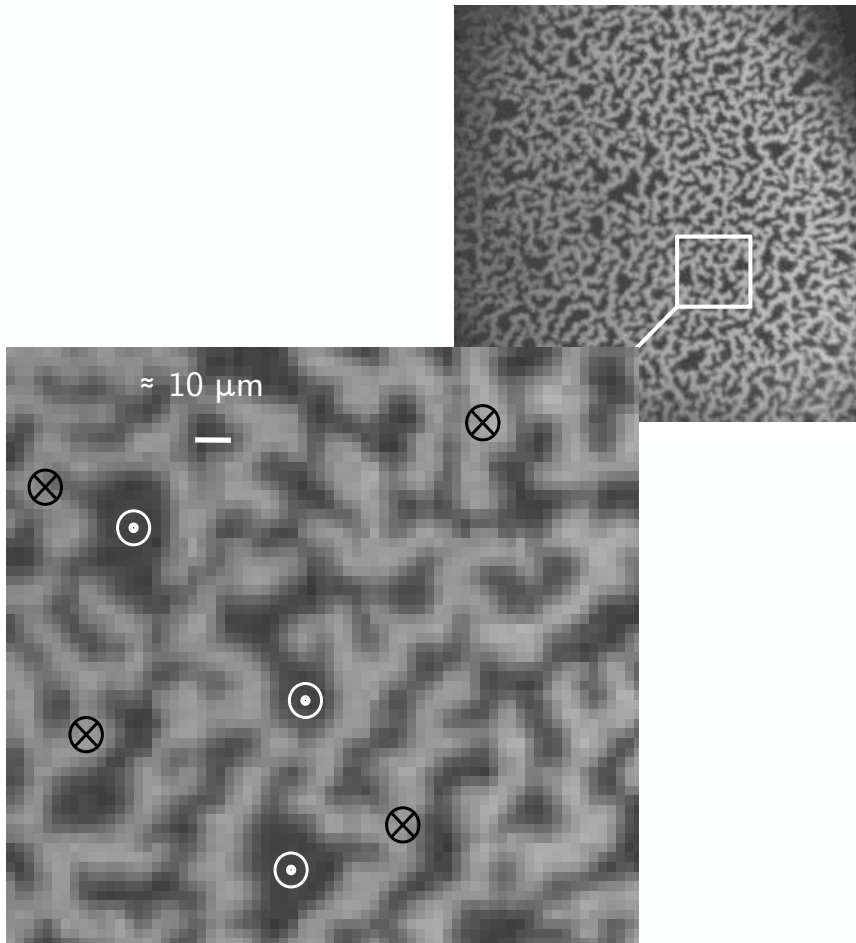
Under development: low-temperature NV scanning microscope



Nanodiamond on tip

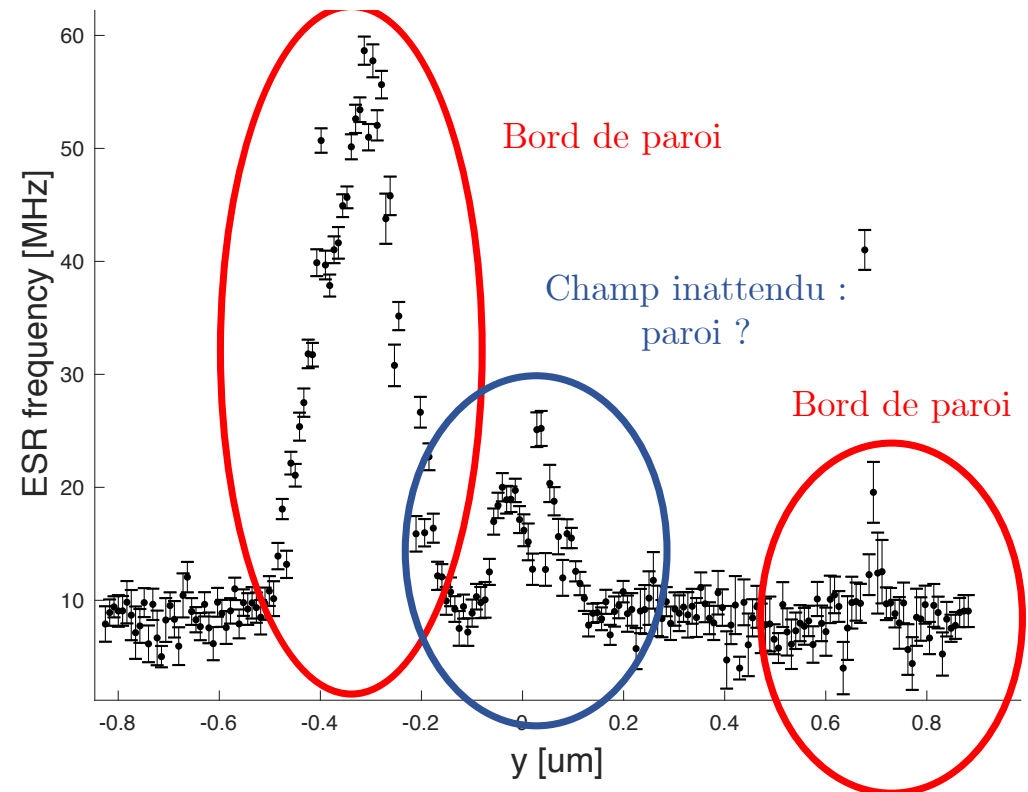
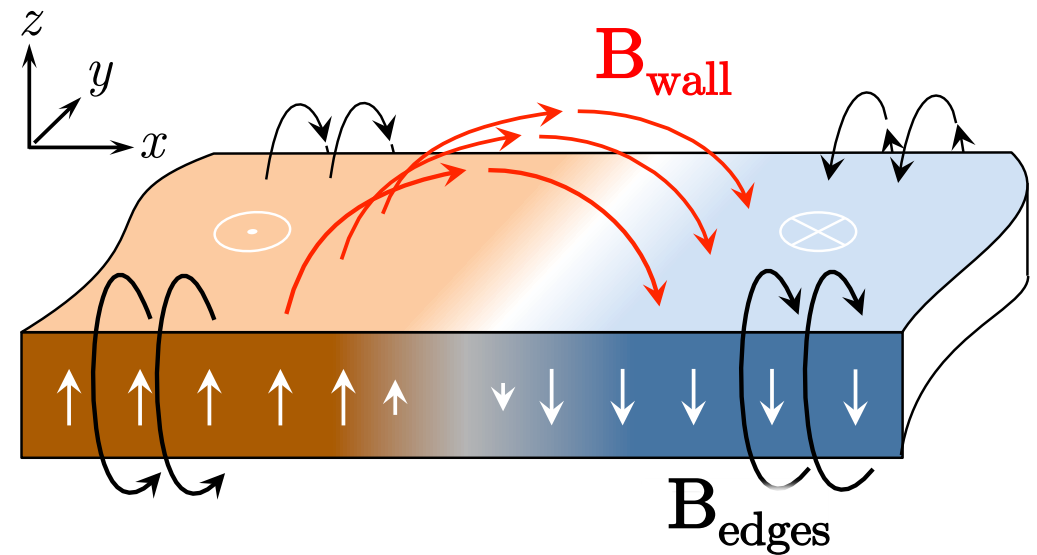


Domain wall imaging at 4 K : GaMnAsP

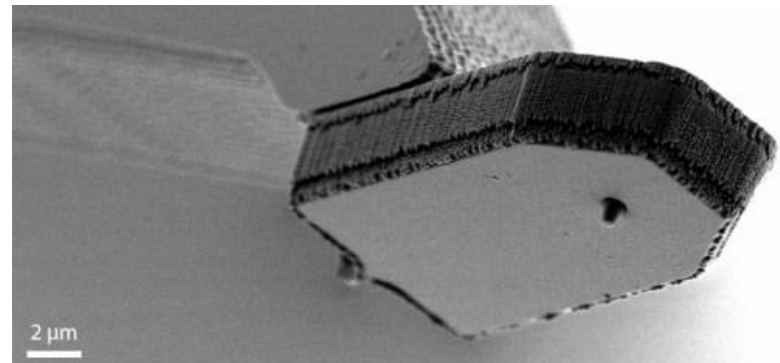
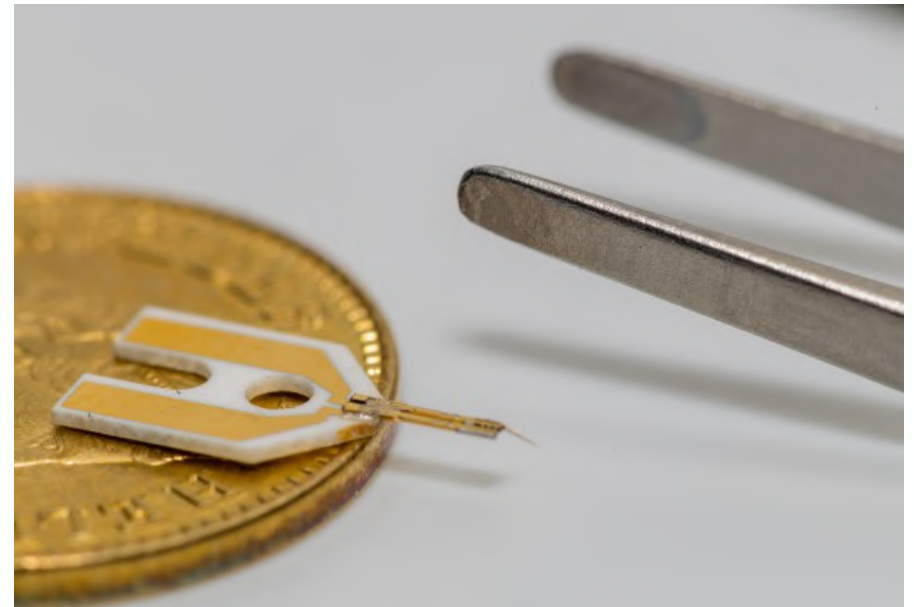
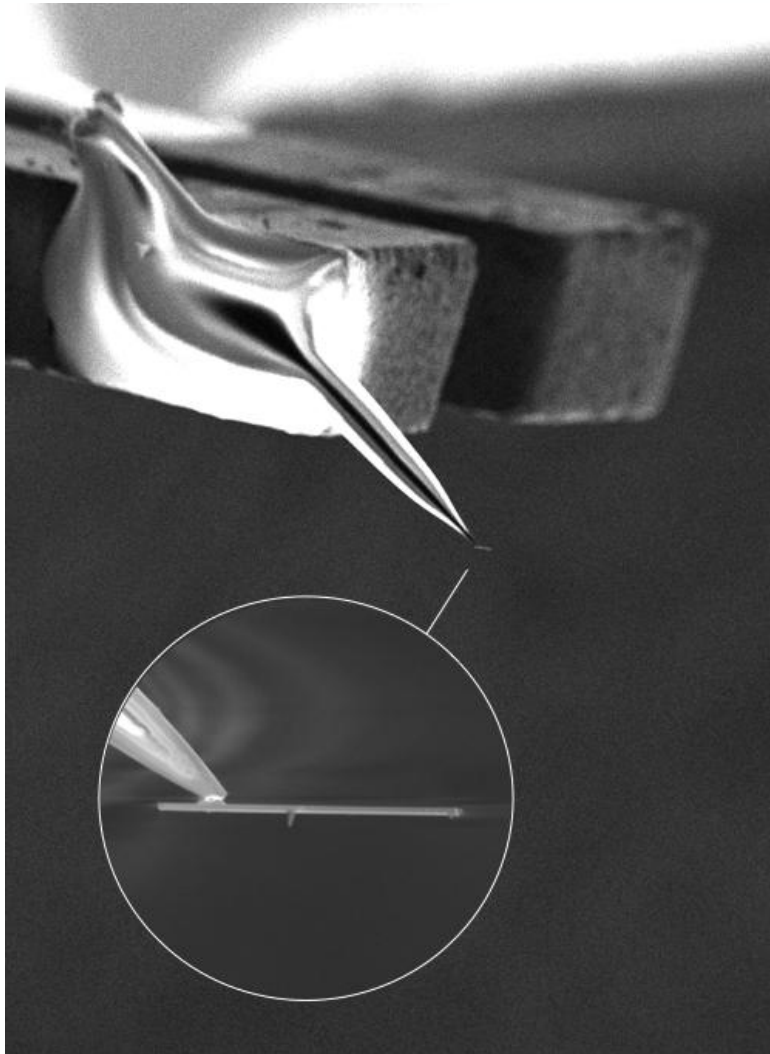


Sample fabricated by
Aristide Lemaître (C2N)

Kerr microscope imaging
by Vincent Jeudy (LPS)



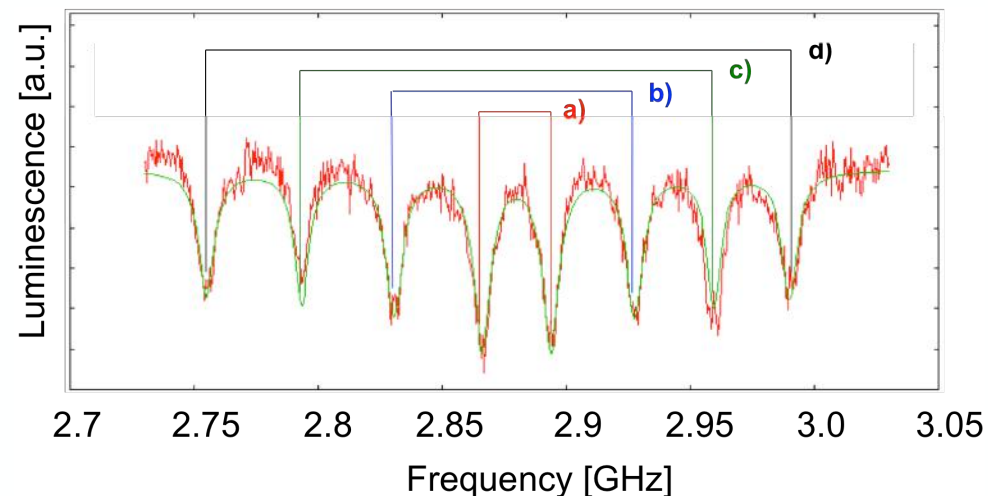
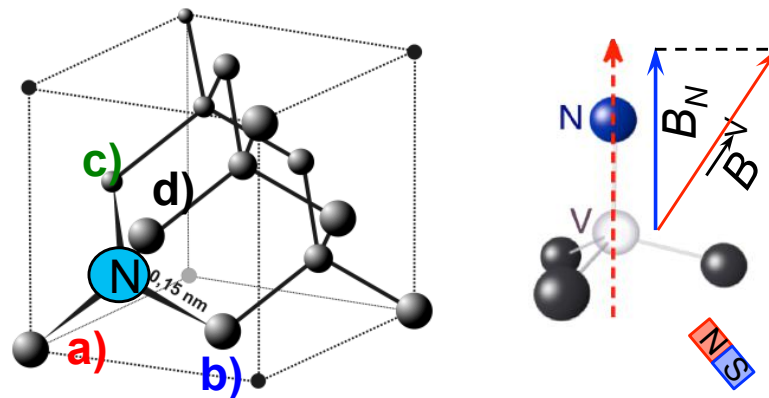
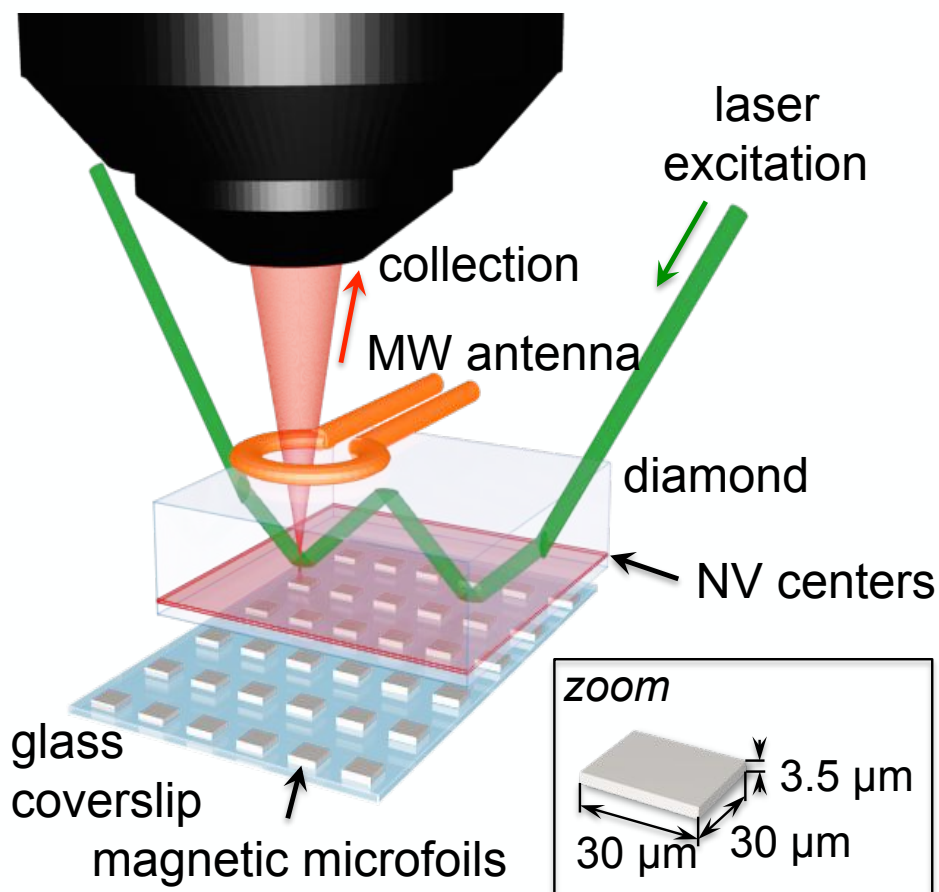
Now (almost) commercial diamond tips



Wide-field magnetic imaging

CCD camera: Each pixel = 1 magnetic resonance spectrum

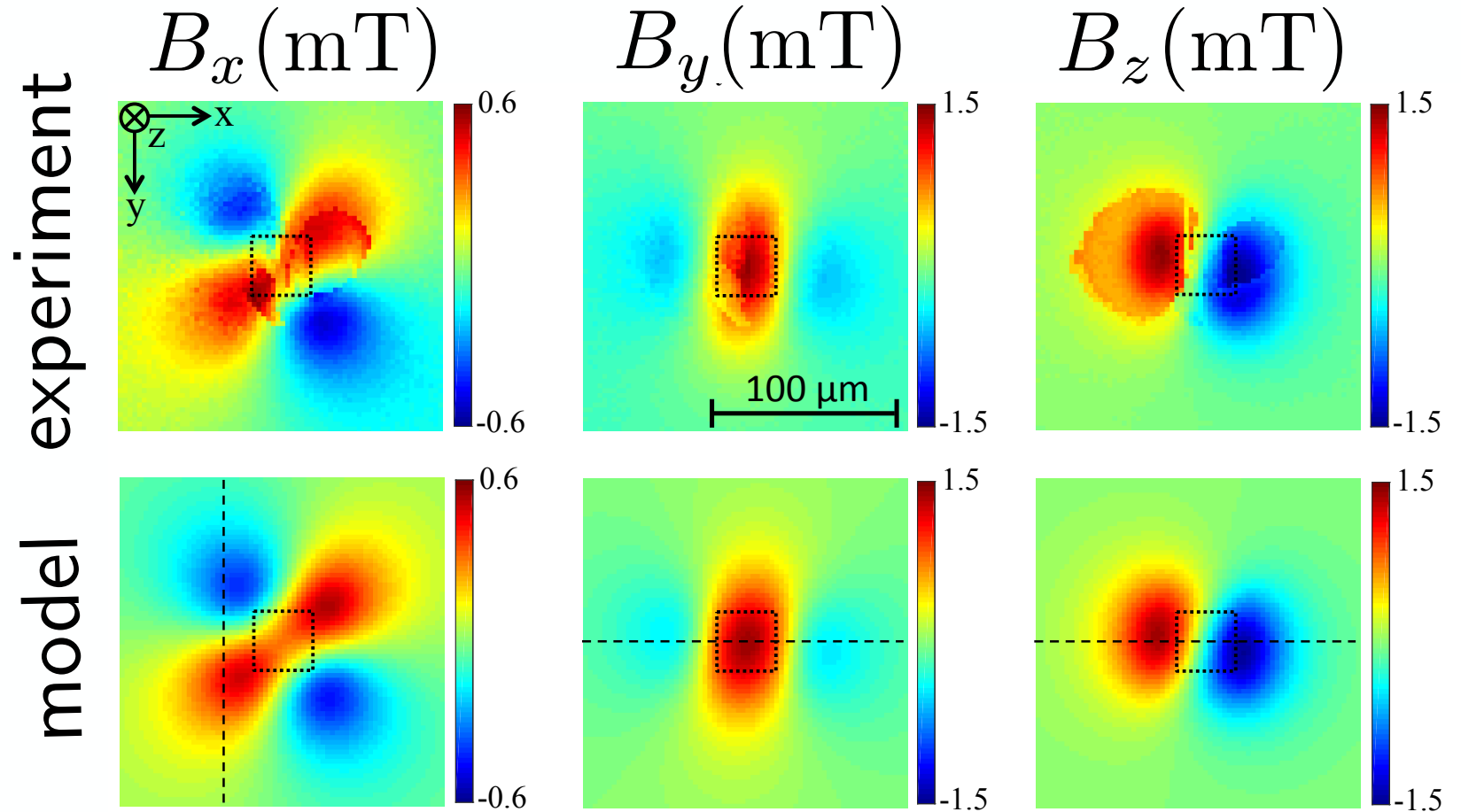
THALES
Th. Debuisschert



set of 4 correlated informations
maximum likelihood $\longrightarrow (B_x, B_y, B_z)$

J. Wrachtrup (Stuttgart), R. Walworth (Harvard)

B-field produced by a permalloy dot



$$M = 7.9 \times 10^4 \text{ A/m}$$
$$z = 19.5 \mu\text{m}$$

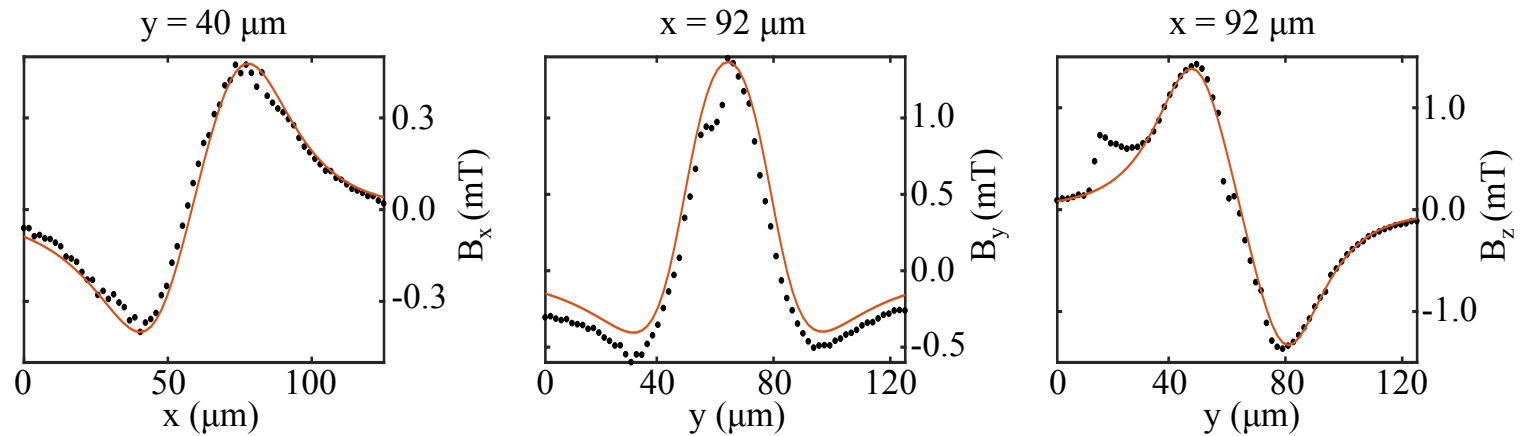
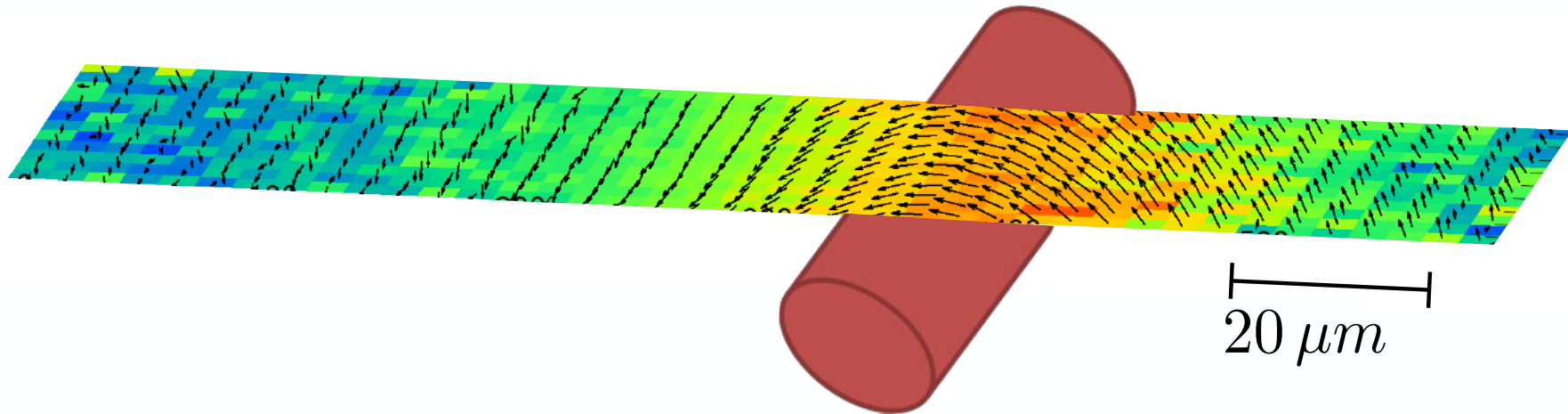


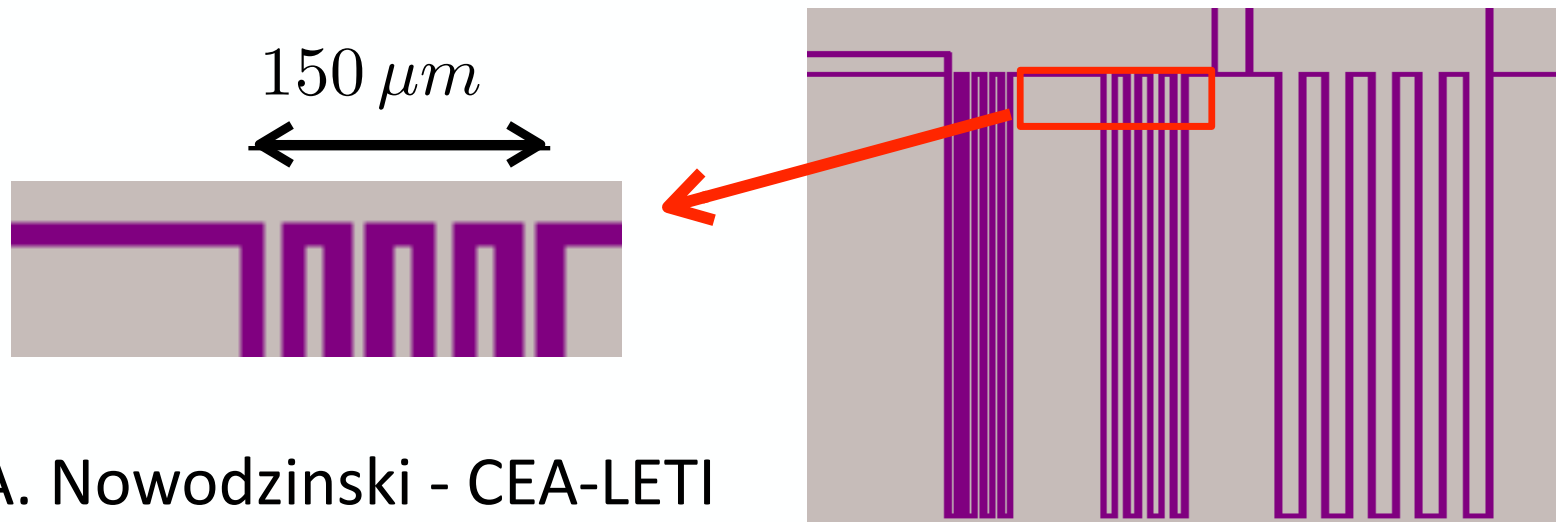
Image of magnetic field distribution

Resolution : standard optical microscopy ~ 400 nm



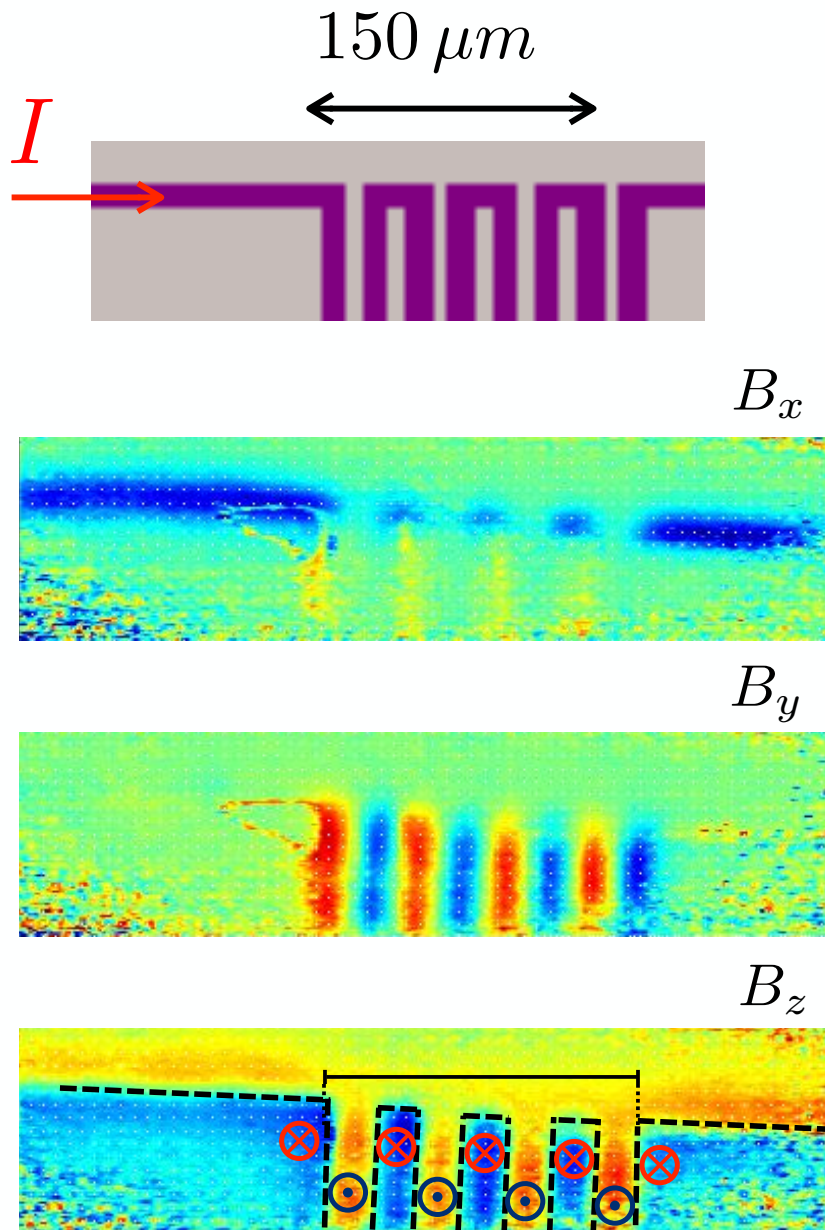
M. Chipeaux et al., Eur. Phys. J. D **69**, 166 (2015)

...can be used to retrieve a current distribution
in microelectronics



Coll. A. Nowodzinski - CEA-LETI

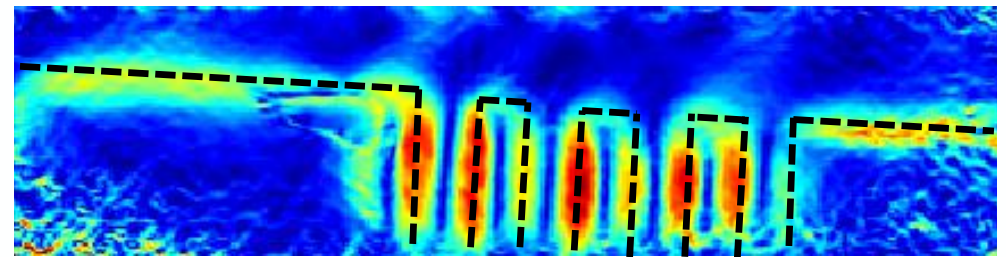
Mapping current density in microelectronics



$$\vec{B}(\vec{r}) = \frac{\mu_0}{4\pi} \int \frac{\vec{j}(\vec{r} - \vec{r}') \times (\vec{r} - \vec{r}')}{|\vec{r} - \vec{r}'|^3} d^3 r'$$

Biot-Savart law can be inverted by FT
unicity of solution for 2D current

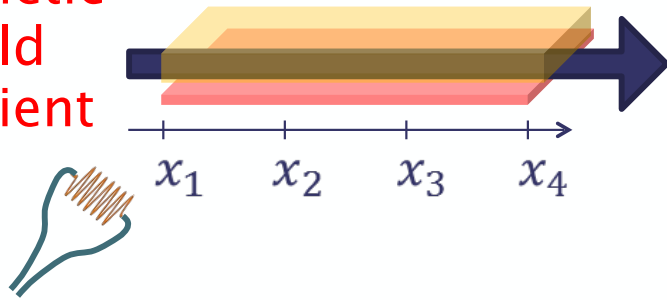
→ map of $\|\vec{j}(\vec{r})\|$



Spatial resolution on \vec{B} measurement
has a key influence on the accuracy
on the \vec{j} reconstruction

NV center = magnetometer and reciprocally it is also a microwave spectrum analyzer

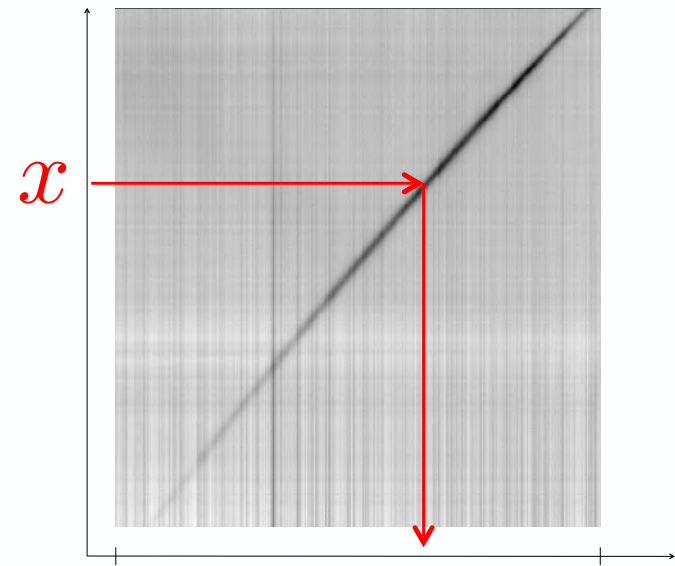
Magnetic field gradient



Correspondance between MW frequency and position
M. Chipeaux et al., Appl. Phys. Lett. 107, 233502 (2015)

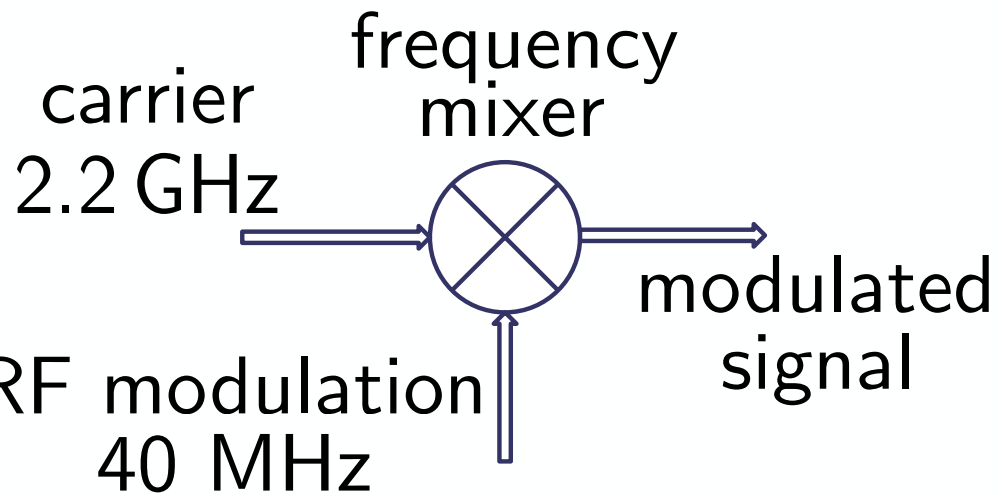
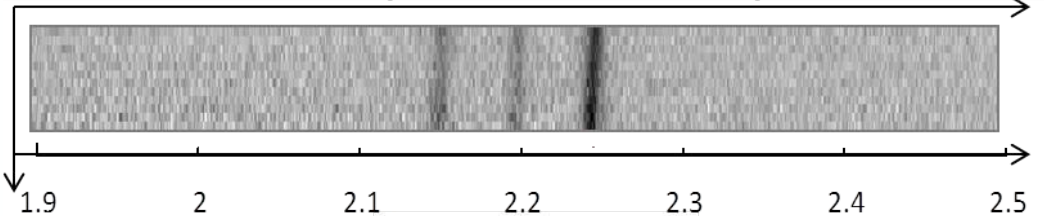
T. DEBUISSCHERT et L. MAYER

THALES

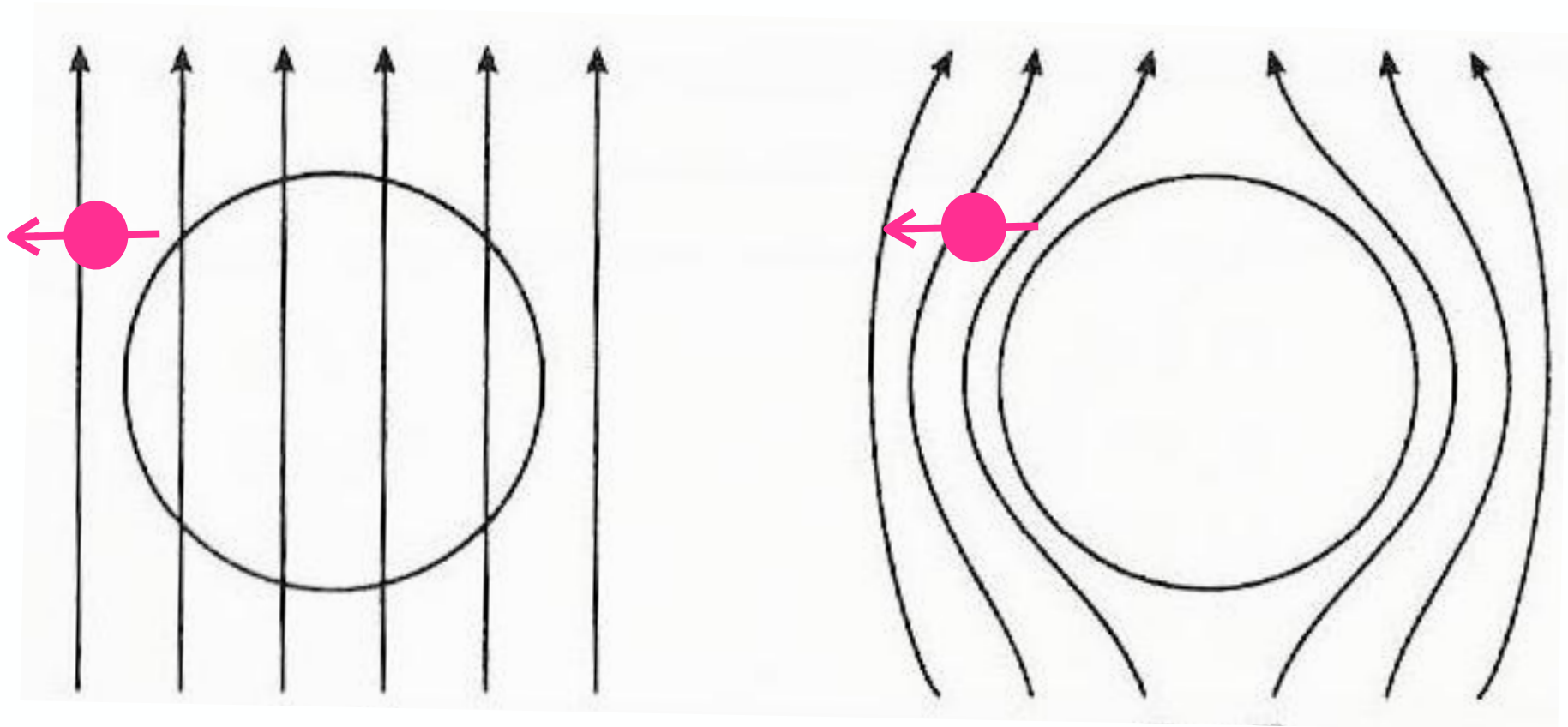


1.85 GHz ν 2.55 GHz

axis of magnetic field gradient



NV-based diagnostic of superconductivity: Observation of the Meissner effect



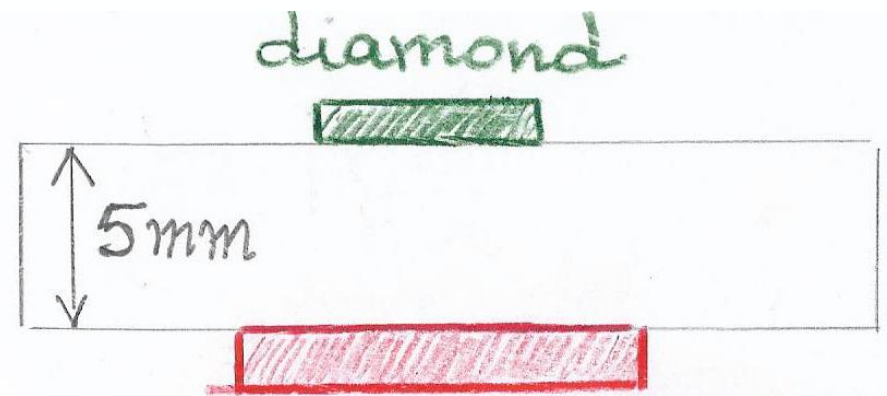
$$T > T_c$$

$$T < T_c$$

Detection of the Meissner effect with a diamond magnetometer

Louis-S Bouchard^{1,3}, Victor M Acosta², Erik Bauch²
and Dmitry Budker²

New Journal of Physics **13**, 025017 (2011)



BSCCO ($T_C = 105$ K)

- Diamond with (111) orientation
- Three Lorentzian resonances (hyperfine coupling with ^{14}N)
- Zeeman shift (Meissner) competes with temperature shift

